

DEPOSITIONAL AND DIAGENETIC CHARACTERISTICS OF A  
PHYLLOID ALGAL MOUND, UPPER PALO PINTO FORMATION,  
CONLEY FIELD, HARDEMAN COUNTY, TEXAS

A Thesis

by

STEPHEN EDD LOVELL

Submitted to the Office of Graduate Studies of  
Texas A&M University  
in partial fulfillment of the requirements for the degree of  
MASTER OF SCIENCE

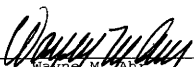
December 1988


Major Subject: Geology

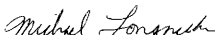
DEPOSITIONAL AND DIAGENETIC CHARACTERISTICS OF A  
PHYLLOID ALGAL MOUND, UPPER PALO PINTO FORMATION,  
CONLEY FIELD, HARDEMAN COUNTY, TEXAS


A Thesis  
by  
STEPHEN EDD LOVELL

Approved as to style and content by:

  
Wayne M. Ahl  
(Chair of Committee)

  
Robert R. Berg  
(Member)

  
Michael T. Longnecker  
(Member)

  
John H. Spang  
(Head of Department)

December 1988

## ABSTRACT

Depositional and Diagenetic Characteristics of a  
Phylloid Algal Mound, Palo Pinto Formation, Conley Field,  
Hardeman County, Texas. (December, 1988)

Stephen Edd Lovell, B.S., University of Texas at Austin

Chair of Advisory Committee: Dr. Wayne M. Ahr

The Palo Pinto Formation is a limestone section rich in phylloid algae, crinoids, bryozoa, molluscs, brachiopods, foraminifera, pellets, intraclasts, oolites, and siliciclastics. Wackestones and bafflestones are most common but packstones, grainstones, and mudstones are also present. Most of the Palo Pinto section displays massive bedding; however, collapse breccias, mottled bedding, and small scale planar cross beds are also present.

Four lithofacies found to represent the Palo Pinto Formation were identified by grouping compositional data observed in core and thin sections. The lithofacies are (from bottom to top): 1) crinoid-shale wackestone; 2) skeletal wackestone; 3) algal bafflestone; and 4) fusulinid-oolite packstone. The crinoid-shale wackestone represents the intermound deposit between carbonate buildups. The skeletal wackestone represents the initial substrate for algal mound growth. The algal bafflestone represents in situ growth of the algal mound. The

fusulinid-oolite packstone is the stratigraphic top of the sequence and represents the end of a shoaling upward phase of deposition.

The buildup at Conley field is 300 - 400 ft (91 - 122 m) thick over a pre-Palo Pinto high which localized reef growth. The reef is circular with a steep side to the north. The present structural crest coincides with the isopach thick of the reef.

Porosity in the upper Palo Pinto Formation is the result of depositional and subsequent diagenetic processes. The highest porosity is in the grainiest facies; however, only a portion of the primary porosity was preserved. Early stage dissolution by undersaturated pore fluids greatly increased porosity. The location of the diagenetic enhanced porosity was controlled by facies locations and topography present during deposition of the algal mound. The most extensive dissolution and consequently the largest porosity, is located in the grainiest facies at paleostructural highs.

## ACKNOWLEDGEMENTS

First and foremost, I would like to thank Dr. Wayne Ahr. His knowledge and enthusiasm for carbonate geology was an inspiration to me during my stay at Texas A&M University. In addition, his constant insistence on quality research improved this thesis. I owe much to my other professors at Texas A&M; most especially, Dr. Robert Berg. I will carry his sense of humor and practical approach to geology into my future work. Dr. John Spang was instrumental in providing me financial aid while at the university.

Shell Oil Company provided two cores used in this study. Sage Energy Company provided a core and recent well logs for Conley field and their cooperation is appreciated.

The drafting of figures in this thesis was done by Mr. Tom Byrd and Mr. Mike Walcher. I am indebted to them for their advice and assistance.

Special thanks goes to my fellow graduate students at Texas A&M. They made my return to school easier and more enjoyable. In particular, thanks to Joel Baker, Tom Byrd, Sheila Gormican, Lynn Travis, Becky Miller, and David Work.

Finally, I could not have returned to school and finished graduate work without love and support from my parents. Their belief in me keeps me going.

## TABLE OF CONTENTS

	PAGE
INTRODUCTION .....	1
The Study Area .....	2
Drilling History .....	2
OBJECTIVES .....	7
BACKGROUND .....	8
GEOLOGIC SETTING .....	12
Regional Structure .....	12
Local Structure .....	14
Stratigraphy .....	15
METHODS .....	18
PALO PINTO ROCK PROPERTIES .....	23
Composition .....	23
Texture .....	26
Sedimentary Structures .....	26
DEPOSITIONAL HISTORY .....	32
Lithofacies Description .....	32
The Reef .....	46
DIAGENESIS .....	61
THE RESERVOIR .....	73
CONCLUSIONS .....	82
REFERENCES CITED .....	84

## TABLE OF CONTENTS (continued)

	PAGE
APPENDIX A: WELL DATA BASE .....	89
APPENDIX B: CORE DESCRIPTIONS AND PETROGRAPHIC DATA ..	93
APPENDIX C: ABBREVIATIONS AND FORMULAS .....	108
VITA .....	111

## LIST OF FIGURES

FIGURE	PAGE
1	Location map of north Texas illustrating the location of the Hardeman basin and surrounding structural features ..... 4
2	Stratigraphic column of the upper Paleozoic section in the Hardeman basin ..... 16
3	Location of wells utilized in the Conley field study ..... 20
4	Core photographs of sedimentary structures from the Palo Pinto Formation ..... 29
5	Bar graph illustrating the distribution of grain types from the Shell Conley 4 well .. 35
6	Bar graph illustrating the distribution of grain types from the Shell Conley 7 well .. 37
7	Core photographs of lithofacies identified from the Palo Pinto Formation ..... 39
8	Well logs from the Shell Conley 7 well ..... 42
9	Isopach map of the Palo Pinto Formation ..... 48
10	Interval isopach map of the shale interval underlying the Palo Pinto Formation ..... 50
11	Present structure on top of the Palo Pinto Formation at Conley field ..... 52



## LIST OF FIGURES (continued)

FIGURE		PAGE
12	North-south stratigraphic cross section A-A' illustrating lithofacies distribution across Conley field .....	55
13	Interval isopach map of the shale interval overlying the Palo Pinto Formation .....	57
14	Structural cross section A-A' illustrating lithofacies distribution and relationship to present day structure .....	60
15	Bar graph illustrating diagenetic features identified from the Shell Conley 4 well .....	63
16	Bar graph illustrating diagenetic features identified from the Shell Conley 7 well .....	65
17	Photomicrographs of diagenetic features from the Palo Pinto Formation .....	70
18	Relationship between porosity, permeability, fluid saturations, and lithofacies from the Shell Oil Conley 7 well .....	77
19	Net pay isopach map of the productive Palo Pinto Formation .....	80

## LIST OF TABLES

TABLE		PAGE
1	Lithofacies and their associated rock properties of the Palo Pinto Formation at Conley field .....	33
2	Summary of initial reservoir properties for the productive Palo Pinto interval at Conley field .....	74
3	Production history for Conley (Palo Pinto) field, Hardeman County, Texas .....	75

## INTRODUCTION

Many Pennsylvanian deposits in the American southwest consist largely of carbonate sediments. Differences between these carbonate deposits are the result of different environments of deposition, diagenetic processes, and tectonic activity. A thorough understanding of the rock properties (composition, texture, and sedimentary structures) and depositional morphology is necessary in order to understand the environment in which these sediments were deposited.

This study focuses on subsurface carbonate rocks from Conley field in the Hardeman basin of north Texas, a site of thick accumulations of carbonate and clastic sediments of Pennsylvanian age. The study of these rocks has led to new knowledge of depositional regimes present in the basin and, as these deposits have economic significance as oil and gas reservoirs, this study has shed light on methods for further hydrocarbon exploration.

---

This thesis follows the style and format of the American Association of Petroleum Geologists Bulletin.

### The Study Area

The Hardeman basin is approximately 11,655 km<sup>2</sup> (4500 mi<sup>2</sup>) in area and encompasses eight counties in southern Oklahoma and northern Texas (Figure 1). The basin is bordered by the Red River-Matador arch to the south, the Wichita uplift to the north, and the shallower Palo Duro basin to the west. The axis of the basin is elongate northwest to southeast and its long axis parallels the present-day Red River. A horst formed during the Precambrian by basement faulting separates the Hardeman basin from the shallower Hollis basin to the north.

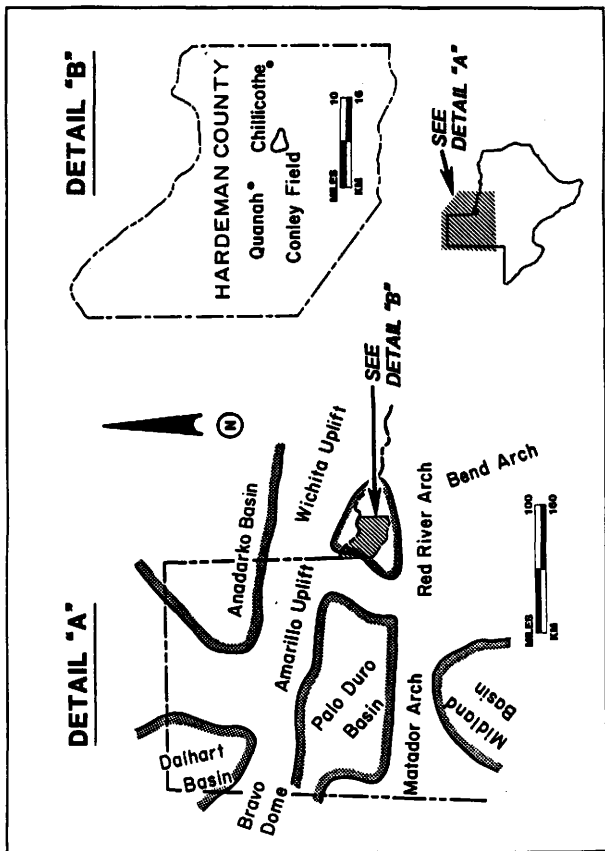
Conley field is located in Block H of the Waco and Northwestern Railroad Company Survey in Hardeman County, Texas. It is positioned midway between the towns of Quanah and Chillicothe near US highway 287 (Figure 1).

### Drilling History

Seismic surveys began in the Hardeman-Palo Duro basin region in 1929 and led to discovery of Altus field. Today there are approximately 130 oil and gas fields in Hardeman County, Texas. Historically, the principal exploration target in the Hardeman basin has been Mississippian carbonate buildups in the Chappel Formation; however, production has been established in Ordovician,



Figure 1. Location map of north Texas illustrating the location of the Hardeman basin and surrounding structural features.



Mississippian, and Pennsylvanian strata. Production from Pennsylvanian rocks occurs primarily in the central and eastern portions of Hardeman County.

Before the discovery of Conley field in 1959, only one successful well and 40 dry holes had been drilled in the basin (Oil and Gas Journal, 1961). Initial exploration at Conley field was conducted by the Amerada Petroleum Company prior to 1939 (Freeman, 1964) and resulted in the Amerada Rice 1 well. This well had a total depth of 8255 ft (2517 m) and penetrated the Ordovician Ellenburger dolomite. A second well was drilled in 1944, but was abandoned. The discovery well for Conley field was the Shell Conley 1. It was drilled in 1959 and had an initial production of 226 BOPD from Mississippian aged rocks. The first Palo Pinto production in the field began in 1963 from the Shell Conley 3. Production at Conley field has been from Ordovician (Ellenburger Formation), Mississippian (Osage and Chappel Formations), and Pennsylvanian (Palo Pinto Formation) strata.

Conley South field is located approximately four miles south of Conley field. Mississippian production was established in 1966; however, the wells were plugged and abandoned in 1970. Production from the Pennsylvanian section was established in 1984 and the field currently produces from Pennsylvanian carbonates. To date, no detailed studies of the reservoir rocks in the field have been published.

Conley North field was discovered in 1968 and is



located 3.75 miles north of Conley field. Similar to the Conley South field, initial production was from the Mississippian section with Pennsylvanian production beginning in 1985. The shallowest production was reported from the Palo Pinto "sand". This sand is stratigraphically 700 ft (213 m) below the Palo Pinto limestone at Conley field and may actually correlate with the Mississippian, Chester sand.

## OBJECTIVES

The purpose of this study is to determine the depositional and diagenetic history of the Palo Pinto Formation at Conley field. The principal objectives of this research are:

- 1) To define the environment of deposition of the upper Palo Pinto limestone.
- 2) To describe the categories of diagenesis and tabulate their relative abundance and distribution.
- 3) To compare the present porosity distribution with the depositional and diagenetic characteristics of Palo Pinto rocks at Conley field.

## BACKGROUND

The Pennsylvanian equator extended diagonally northeast-southwest across North America (Wilson, 1975). Pennsylvanian times are characterized by cyclical deposits of carbonates and terrigenous clastics. Carbonate buildups have been identified from the subsurface of west Texas (Schatzinger, 1983; Toomey and Winland, 1973), the Paradox basin (Choquette, 1983; Wilson, 1975; Peterson, 1959), and in outcrop in the Sacramento Mountains (Wilson, 1975; Toomey et al, 1977). These carbonate buildups typically show relief of 80-330 ft (24-101 m) and have flanking beds which dip as much as 25° (James, 1983; Toomey and Winland, 1973). Despite differences in size and shape, the buildups share common lithofacies and exhibit extensive vertical and lateral thickening as compared to the surrounding intermound deposits.

The thickest buildups developed in deeper water settings apart from more extensive carbonate deposition on shelf margins. These isolated banks and mounds grew in areas of rapid subsidence where only the highest areas remained in the photic zone (Wilson, 1975). Nena Lucia field, Nolan County, Texas is part of a series of north-south trending carbonate banks located on the eastern side of the Midland basin. The buildup is elongate in shape and trends northeast-southwest. A study by Toomey and Winland (1973)

attempted to distinguish laterally equivalent facies so that with limited well data proximity and direction to the reef could be discerned. Although facies could be distinguished, the amount of variation was too small to determine proximity to the reef. Six carbonate facies and two terrigenous clastic facies were identified. A similar study was done on the Kelly-Snyder field, west Texas, where facies changes in a mound-to-basin tract through the eastern portion of the "Horseshoe Atoll" were described (Schatzinger, 1983).

Upper carboniferous reefs in the Sacramento Mountains grew on a northwest-southeast trending shelf margin (Wilson, 1975). The reefs grew as a linear chain with biohermal axes parallel to depositional strike. The reefs and associated flank beds consist of a progression of down-to-the-basin offlapping growth stages (Toomey et al, 1977). Most studies have focused on the Yucca mound complex, a reef which attained a total height at the end of its latest growth stage of approximately 80 ft (24 m). Similar to the Nena Lucia buildup, Yucca Mound has a phylloid algal core facies. This algal facies displays a collapse breccia structure and is overlain by a capping, boundstone facies. Yucca Mound represents vertical growth into progressively shallow water and under the influence of waves and currents. An estimated water depth of approximately 100 ft (30 m) for the intermound areas at Yucca Mound was established by Toomey et al (1977).

Phylloid algal mounds in the Paradox basin have been described in detail because they are prolific oil and gas reservoirs. In his early work, Peterson (1959) described four Pennsylvanian-aged facies referring to one as the "shelf or platform carbonates". This facies includes biohermal carbonates described as "reefy" buildups which consist of fossil debris of Desmoinesian age. The oldest buildups are present to the southwest and are composed of tubular foraminifera and plumose algae (Wilson, 1975). Phylloid algae are conspicuously absent in these older, southwestern buildups. Wilson (1975) interpretes this assemblage as a downslope accumulation on a steep shelf. He states that it is similar to facies which cap platy algal mounds in later Pennsylvanian rocks. Younger subsurface bioherms are located to the northeast (basinward) of the older buildups. Producing fields from the younger buildups include Aneth, Ismay, Desert Creek, Tin Cup Mesa, Barker Dome, and White Mesa. Choquette (1983) states that these younger reef mounds are generally flat-bottomed and have approximately 98 ft (30 m) of depositional relief. Slopes can be 25-30° on the flanks of the mounds. The facies identified within the mounds have a characteristic cyclic pattern (Choquette, 1983). Features indicative of subaerial exposure, such as mud cracks, fenestral fabrics, and solution porosity, are present at the end of these cycles. The mounds have capping facies composed of oolites and

fusulinids with intermound deposits of fine-grained mudstones rich in crinoid fragments and sponge spicules (Herrod et al, 1985 and Choquette, 1983). Choquette and Trout (1963) stated that the amount of platy algae in the Ismay buildup increases up section. Syndepositional collapse breccias are commonly found in the Paradox basin mounds. They are located in the mound core but can also be associated with flanking facies (Herrod et al, 1985). In contrast to mounds elsewhere in the southwest, many Paradox basin algal mounds are oriented with their long axes at right angles to depositional strike (Wilson, 1975). Wilson interpretes this to be the result of differences in hydrodynamic conditions present during deposition of the carbonates.

Phylloid algal mounds in the southwest are found in many paleoenvironmental settings ranging from near shore shelf to more basinal settings. Thicker buildups tend to be located in basinal areas. Most of the buildups have 1) a mound "core" facies dominated by phylloid algae and lime mud; 2) a mound capping facies of foraminifera and coated grains; and 3) an intermound facies of fine grained mudstones with crinoid fragments and sponge spicules as dominant grain types. The mound core facies often contains syndepositional collapse breccias.

## GEOLOGIC SETTING

The Hardeman basin of Texas and southern Oklahoma is located in a region where tectonism was important in shaping the area. The basin configuration resulted from both tensional and compressive stresses caused by tectonic events mainly during the Mississippian and Pennsylvanian periods.

### Regional Structure

Rifting of the Late Proterozoic North American continent subjected the southern margin of North America to tensional stresses and resulted in the formation of a proto-Gulf of Mexico (Iapetus Ocean). Orthogonal "bends" in this continental margin have been explained as being either arms of failed aulacogens (Walper, 1977) or the result of offsets along transform faults (Thomas, 1985 and King, 1975). These Precambrian fault complexes were zones of weakness which were later reactivated during Mississippian and Pennsylvanian periods.

Rocks of Cambrian to Early Mississippian age indicate deposition along a passive continental margin (Thomas, 1985). Walper (1977) and Keller and Cebull (1973) postulated that an early Paleozoic subduction zone and associated arc-trench system existed off the southern margin of North America. This system is not interpreted to have

affected the more stable, continental shelf.

Walper (1977) proposed that a reversal in subduction polarity occurred during Silurian and Devonian times. The resultant change in stress patterns across the Texas-Oklahoma area led to the closure of the marginal basin which existed between the continental shelf and the offshore arc. Compressive stresses generated by this plate convergence were transmitted to the interior of the continent along the boundary faults of pre-existing aulacogens (Walper, 1977), resulting in the formation of paired uplifts (Amarillo-Wichita uplifts) and basins (Anadarko, Ardmore, and Hardeman basins). These features are elongate in the direction of the principal compressive stress (northwest-southeast). The only structural feature in north Texas which does not follow this northwest-southeast trend is the Red River-Matador arch. The arch trends east-west and merges with the Amarillo-Wichita uplift on the east side of the Hardeman basin. The east-west orientation of this trend could have resulted from ductility contrasts between the Tillman Metagreywacke province (Red River-Matador arch) and surrounding granitic terrain (Flawn, 1956 and Montgomery, 1984).

The north Texas-southern Oklahoma area remained quiet tectonically throughout the Mesozoic and Cenozoic except for the opening of the Gulf of Mexico during the Jurassic. This later tectonic activity did not mask the



affects of previous tectonic events.

#### Local Structure

The Hardeman basin is a graben present at the juncture of the Amarillo-Wichita and Red River-Matador fault zones. Initially, these fault systems were created by Precambrian-Cambrian rifting. A horst of approximately 1000 ft (300 m) separates the Hardeman basin from the Hollis basin (Oklahoma) (Montgomery, 1984). These two features exist as separate lows within the same graben.

The northern portion of the Hardeman-Hollis basin is bounded by the Burch Fault, a steep, north-dipping, reverse fault which developed along the northern margin of the late Precambrian basin (Montgomery, 1984). The Hardeman basin is bounded by the Red River-Matador arch on the southeast and to the southwest the basin is characterized by gentle dips with little or no faulting.

Information about the basement and faults is limited in the Hardeman basin area. Montgomery (1984) states that industry geologists map high angle faults which extend into the axis of the basin. These faults have a maximum of 394 ft (120 m) of vertical displacement and change from a northwest-southeast orientation in the north to an east-west orientation to the south. This orientation conforms to the regional structural trend.

Budnik (1983) showed that northwest trending faults in the Palo Duro basin converge to the Amarillo uplift. These faults have limited vertical displacements and overlying strata exhibit only minor drape folding. A similar fault trend exists in Childress, Hall, and Donley counties west of the Hardeman basin (Goldstein and McGookey, 1982). The faults are vertical reverse faults with a small amount of right lateral displacement. They penetrate the entire Paleozoic section. It is not known if similar style faulting is also present in the Hardeman basin.

#### Stratigraphy

Paleozoic stratigraphy of north-central Texas was initially studied by Tarr (1890) and Cummins (1891) who assigned stratigraphic names to Pennsylvanian rocks in the coal fields of the Colorado and Brazos River valleys. Their terminology has been modified by various authors and a synopsis of the current terminology is given by Erxleben (1975).

Stratigraphic nomenclature in the Hardeman basin is the same as that of the Eastern Shelf of Texas. Most work done on Hardeman basin rocks are oil field studies which do not include regional stratigraphic correlations. A stratigraphic column of the upper Paleozoic section in the Hardeman basin is shown in Figure 2.

SYSTEM	SERIES	GROUP	FORMATION (HARDEMAN BASIN)
PERMIAN	WOLFCAMPIAN	WICHITA-ALBANY	COLEMAN JUNCTION
			DOTHAN IBEX
PENNSYLVANIAN	VIRGILIAN	CISCO	NOBLE / BUNGER
	MISSOURIAN	CANYON	PALO PINTO
		STRAWN	CADDO
	ATOKAN	? — ? BEND	? — ? BEND
	MISSISSIPPIAN	CHESTERIAN	CHESTER
MERAMECIAN		MERAMEC	ST. GENEVIEVE
			ST. LOUIS
		OSAGE	CHAPPEL

Figure 2. Stratigraphic column of the upper Palaeozoic section in the Hardeman basin. Compiled from Exleben (1975), Ross (1981), Montgomery (1984), and Ruppel (1984).

Strata in the Hardeman basin are exclusively Paleozoic in age. Rocks of Cambrian, Ordovician and Mississippian age have been identified in the basin. Since Morrowan rocks are absent, the contact between Mississippian and Pennsylvanian age rocks is believed to be an unconformity.

The middle Pennsylvanian was a time of intense tectonism in north Texas. Thick accumulations of clastic sediments were shed from Precambrian basement rocks north and south of the Palo Duro and Hardeman basins (Handford, 1979). These clastics built fan delta complexes contributed a large amount of sediment to the eastern part of the Palo Duro basin. The Hardeman basin received only a minor amount of this clastic deposition. With the exception of some granite wash which occurs near the northern limit of the basin, it was a clastic-free environment. This resulted in thick (2000 feet, 610 m) deposits of carbonates, including phylloid algal buildups (Kerr, 1969), with interbeds of fine grained terrigenous clastics. Overlying the Pennsylvanian section is approximately 3000 ft (915 m) of Permian carbonates with interbedded sands and shales.

## METHODS

Cores, borehole logs, scout tickets, and core analyses were utilized in this study. Cores from two wells, the Shell Conley 4 and Shell Conley 7, were acquired from Shell Oil Company. A third well, the Sage Conley 17, was obtained from Sage Energy Company. The Conley 7 core is from the center of the field; the Conley 4 and Conley 17 cores are from the edges of the field (Figure 3). The cored intervals include the upper 130 ft (40 m) of the Palo Pinto Formation. A total footage of 280 ft (85 m) of core was examined. The cores were acid-etched and systematically described with a binocular microscope using Dunham (1962) and Embry and Klovan's (1971) classification schemes. Rock properties such as composition, texture, sedimentary structures, and visible porosity were logged. Porosity was classified according to Choquette and Pray (1970). From these data, lithogenetic units were identified. A total of 92 thin sections were made from representative samples of the cored interval from the Conley 4 and Conley 7 wells. Samples were collected at 2-foot intervals.

Constituent composition was obtained by counting 200 points per slide. The presence of dolomite was determined by staining a portion of each slide with an Alizarin Red stain.

Lithofacies were constructed by defining boundaries between grouped compositional data. The grouping was done by



Figure 3. Location of wells utilized in the Conley field study. Cored wells and cross section locations are indicated. A complete list of wells is included in Appendix A.





making correlation plots (scatter plots) of different grain types. The grain types were paired and their percentages plotted as the x and y axes. A coefficient of correlation ( $r$ ) was calculated from the plots to indicate which compositional components were related. Similar grain types were grouped and boundaries set. These boundaries defined lithofacies. A vertical sequence of lithofacies was indicated by the construction of compositional graphs.

Structure and isopach maps were made from 58 borehole logs. Gamma ray and spontaneous potential logs were used to pick formation tops. These tops were then correlated across the field area from which stratigraphic and structural cross sections were constructed. The structure maps indicated the shape of present-day structure and the isopach maps indicate paleo thicks and thins which indicate, in turn, paleostructures. Logs were also used to define the lateral extent of lithofacies. This was done by matching the vertical sequence of lithofacies from the two cored wells to gamma ray and acoustic log curves. The log curves were then correlated to adjacent wells. Lithofacies patterns were added to structural and stratigraphic cross sections. A list of wells used in this study is contained in Appendix A.

The diagenetic history of the cored interval was determined by identifying diagenetic categories. The relative abundance of each category was obtained by estimating the percentage of the category on each thin

section. Vertical bar graphs were constructed for the cored wells in order to compare diagenetic features to lithofacies.

Porosity values were calculated from acoustic well logs. The formula used to calculate porosity is included in Appendix C. The accuracy of the values were compared to core analysis from the Conley 7 well. The extent to which porosity was the result of depositional or diagenetic events was determined by the construction of x-y cross plots. Percentages of a particular grain type was plotted against the percentage of porosity. This was done for all grain types as well as diagenetic categories.

A net pay isopach map was constructed from acoustic logs by totaling the number of feet with porosity greater than 5%. This was done above the reported oil/water contact for the Palo Pinto formation. A comparison was done between this map and present-day structure and post-Palo Pinto paleostructure.

## PALO PINTO ROCK PROPERTIES

## Composition

The principal constituents of the upper Palo Pinto Limestone are phylloid algae, crinoids, bryozoa, molluscs, brachiopods (shells and spines), foraminifera, and ostracods. Non-skeletal grains include pellets, intraclasts, oolites, and siliciclastics. The grains are encased in a matrix of lime mud. Core descriptions and thin section point count data are included in Appendix B.

Two types of algae were identified in the cored interval; they include fragments of phylloid algae and minor amounts of coralline red algae. Phylloid algae may be present in any level of the Palo Pinto section and are locally the dominant grain type. Red algae are a minor component and were identified in only one core.

The probable life form of phylloid algae was described by Pray and Wray (1963). This alga was an upright shallow marine plant with individual leaf-like plates. The plant was only a few inches high with the "leaves" or "plates" unable to withstand a high degree of wave turbulence (Toomey and Winland, 1973). These plates were calcified and upon death of the plant, broke into semi-rigid fragments. The plate fragments served as sediment traps for lime mud and other fine to medium sized

particles. While the algae did not provide a rigid framework like modern day reef builders, it was probably a prolific sediment producer in addition to acting as a sediment baffle. The algal plates in the studied sections are so altered that the genera could not be determined. These algae are preferentially found on shelf margins and inner shelf regions of the Lower Permian of the Southern Alps (Flügel, 1978), where their presence is interpreted to indicate growth and deposition in relatively shallow water (less than 90 ft, 30 m). Most algal plates in the Palo Pinto section are not broken.

Echinoderm fragments are present as disarticulated crinoid columnals. The columnals ranged in size from 0.3 to 3 cm in diameter. The fragments were observed over the entire interval and were locally the dominant grain type.

Two varieties of bryozoans, fenestrate and encrusting, were identified. Fenestrate bryozoans were not observed in growth position. Encrusting bryozoans are uncommon and they occur only in a few zones where they were found to encrust phylloid algal plates and shell fragments.

Brachiopod and mollusc shell fragments are present throughout the interval where they occur with a diverse biota. The shell fragments displayed a moderate degree of abrasion or rounding.

Benthonic and planktonic foraminifera are locally common. They are present in a few thin zones where they

were the principal grain type. Benthonic forams may encrust phylloid algal plates and mollusc shell fragments.

Planktonic varieties are present throughout a greater vertical range in the Palo Pinto but usually comprise less than 5% of the total grain count. Two thin zones (less than 1 ft., 0.3 m thick) are dominated by fusulinids.

Pellets are the most common non-skeletal grain type. Alteration of the sediment made identification of these grains difficult; therefore, there may be more pellets in the rocks than were identified. They are most numerous in the muddier intervals which may indicate either lower substrate mobility or presence in a sub-reef environment. Other non-skeletal grain types include intraclasts and oolites. These grains are not present over the entire interval; however, they can be a dominant grain type comprising 90% of the total composition.

Siliciclastics are rare in the Palo Pinto. They are restricted to clay laminae a few centimeters thick and to a single 4 - 12 ft (1 - 4 m) black shale unit. The siliciclastics represent influxes of terrigenes from sources on the edges of the basin.

The composition of the Palo Pinto Limestone is principally a skeletal wackestone. Taxonomic diversity is high with the organisms representing carbonate deposition in a relatively clear water, clastic-free environment.

### Texture

Dunham's (1962) classification scheme were used to distinguish detrital depositional textures in the Palo Pinto Limestone. Embry and Klovan's (1971) classification was used to describe reef rocks. The classification was done by visual inspection of core and thin sections. The rocks studied are primarily wackestones and bafflestones with lesser amounts of packstones, grainstones, and mudstones. The packstones and grainstones are present in all three cores but are limited to 1 - 5 ft (0.3 - 1.6 m) thick zones.

Bafflestone intervals are composed almost exclusively of phylloid algae and lime mud. The packstone and grainstone intervals have intraclasts, oolites, and abraded skeletal fragments as the principal grain types. The taxonomic diversity is highest in the wackestone and packstone intervals.

### Sedimentary Structures

A range in bedding types is present in the Palo Pinto Limestone. A majority of the rock displays massive bedding indicating extensive burrowing of the sediment by marine organisms. This lack of bedding is present primarily

in the wackestone and packstone intervals. Occasional zones display mottled bedding and are present near the top of the cored interval (Figure 4A). This bedding may be the result of burrowing organisms (Flügel, 1982).

Clay laminae structures were described using the classification scheme of Campbell (1967). The laminae display a variety of characteristics including: 1) wavy, nonparallel, discontinuous; 2) even, parallel, continuous, and 3) inclined, subparallel, continuous structures. Crinoid columnals are concentrated along the laminae and accentuate the outline of the structures (Figure 4B). The laminae are thicker and more numerous in the muddier intervals with the continuity of individual laminae interpreted to represent less scour and only moderate bioturbation at the time of deposition.

Grainstone and packstone intervals at the base of the cored interval in the Conley 4 and Conley 17 wells display sets of small scale planar cross laminated sedimentary structures (Figure 4C). The scale of the laminae sets are on the order of 3 in (8 cm). These features result from migration of straight crested ripples (Leeder, 1982).

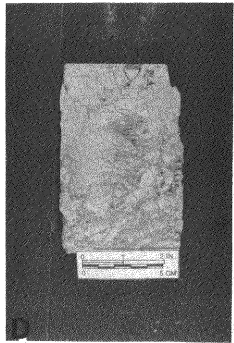
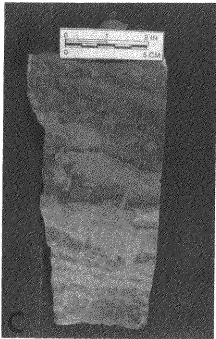
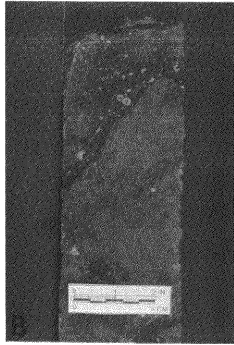
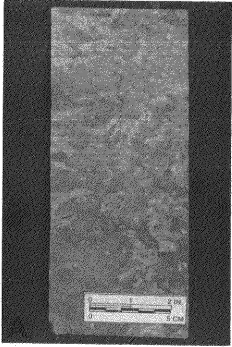
An association exists between sedimentary structures and texture in the Palo Pinto Limestone. The rock with the lowest percentage of lime mud (grainstones and packstones) display the cross laminated structures. The





Figure 4. Core photographs of sedimentary structures from the Palo Pinto Formation.

- A. Predominantly lime mud with a mottled appearance and distinct absence of bedding. (Sage Energy Conley 17, 5226.5 ft.)
- B. Inclined, subparallel, continuous clay laminae from the Shell Conley 7 core. Crinoid columnals typically concentrate along the laminae. (Shell Oil Conley 4, 5214.0 ft.)
- C. Planar cross laminated grainstone partially disrupted by bioturbation. Colletes and fusulinid tests are the principal grain types. (Sage Energy Conley 17, 5241.5 ft.)
- D. Collapse breccia structure. The rock is a wackestone with phylloid algae the primary grain type. (Shell Oil Conley 7, 5258.0 ft.)



mudstones and wackestones display either massive or mottled bedding. These rocks were subjected to the most intense burrowing by marine organisms. Clay laminae structures are also present in the muddier rocks. They are most common in a 4 ft (1 m) section near the top of all three cores.

A portion of the cored interval displays a texture described by various authors as brecciated (Figure 4D). The interval reaches a maximum of 10 ft (3.2 m) thick in the Conley 7 core and is present in all three cores. The rock is classified as a wackestone with phylloid algae as the principal grain type. The brecciated structure indicates that original void space was eliminated by collapse of the sediment. This collapse breccia differs from a true breccia in that there is no evidence of significant transportation. Two prevailing theories could account for the formation of this feature. The first, described by Dunham (1969), attributes the formation to vadose weathering of the rock which produces caverns which subsequently collapse. A second explanation was put forth by Shinn et al (1983) from laboratory experimentation. Their results revealed that early compaction in the marine environment could also cause the brecciated appearance of the rock. This latter theory more realistically describes the type of textures observed in the Palo Pinto limestone at Conley field. The feature appears to be formed by in situ compaction of grain constituents while the sediment was only partially

lithified. Primary void space was reduced upon compaction of the lime mud and phylloid algal grains. The algal grains did not build a rigid framework and upon initial burial, could not support overlying sediment. There is no evidence of transportation of the sediment after deposition. The resulting rock appears to have been deformed in place. The collapse breccia structure is restricted to a single interval composed of phylloid algae and lime mud.

## DEPOSITIONAL HISTORY

## Lithofacies Description

Four different lithofacies were identified in the upper Palo Pinto Formation. The lithofacies boundaries were defined by grouping compositional data observed in core and thin sections. The lithofacies represent the sequential growth of an algal mound and its associated deposits. They also represent a standard sequence for the Palo Pinto Formation. Table 1 lists the lithofacies and their characteristics. Figures 5 and 6 compare the distribution of grain types and assigned lithofacies from the Shell Conley 4 and Shell Conley 7 wells. The lithofacies are:

- 1) crinoid-shale wackestone
- 2) skeletal wackestone
- 3) algal bafflestone
- 4) fusulinid-oolite packstone

Crinoid-shale wackestone lithofacies (Figure 7A).

The most distinctive unit in the cored interval is the crinoid-shale wackestone lithofacies. Lime mud and very fine grained clastics are the principal components of this lithofacies. Grains, including crinoid and bryozoan debris, are typically concentrated along clay laminae and accentuate

Table 1. Lithofacies and their associated rock properties of the Palo Pinto Formation at Conley field.

LITHOFACIES	COMPOSITION Percentage of matrix and principal grain types	TEXTURE	SEDIMENTARY STRUCTURES
FUSULINID-OOLITE PACKSTONE	2-20% foraminifera 0-59% coillies 0-45% lime mud	packstones and grainstones poor to moderate sorting	massive to "wispy" bedding cross bedding in oolitic grainstones
ALGAL BAFFLESTONE	7-30% phyloid algae 26-82% lime mud	wackstones and packstones moderate to good sorting	collapse breccia algal plates horizontal and directionally oriented "clotted" appearance in muddier intervals
SKELETAL WACKSTONE	1-12% echinoderms 2-15% bryozoans 0-16% phyloid algae 23-72% lime mud	wackstone and mudstone poor to moderate sorting	burrowed and reworked mottled bedding laminar-wave to even, subparallel to parallel, continuous to discontinuous
CRINOID-SHALE WACKSTONE	6-32% echinoderms 5-21% bryozoans 27-78% shale and lime mud	wackstones and mudstones poor sorting	burrowed and reworked laminae-even to inclined, parallel to subparallel, continuous



Figure 5. Bar graph illustrating the distribution of grain types from the Shell Conley 4 well.



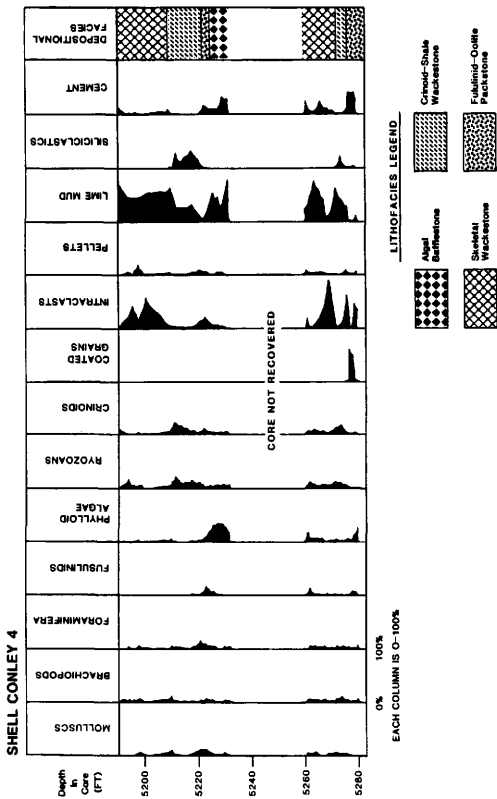




Figure 6. Bar graph illustrating the distribution of grain types from the Shell Conley 7 well. Lithofacies patterns are defined in Figure 5.

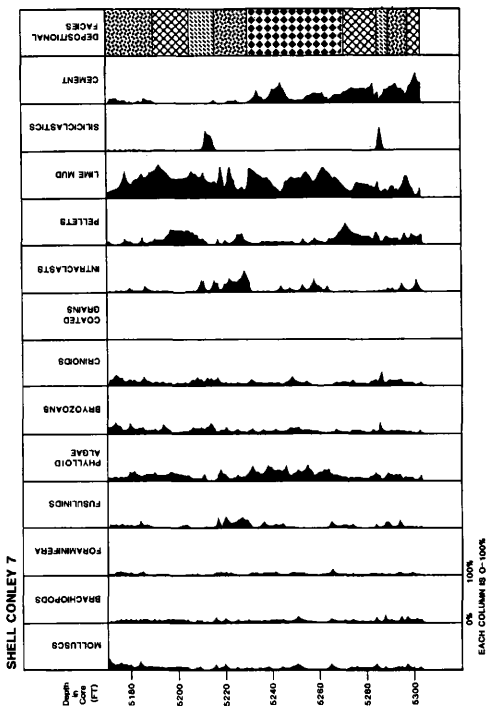
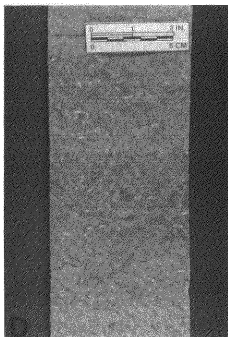
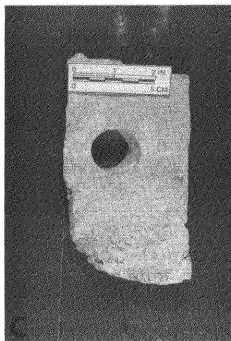
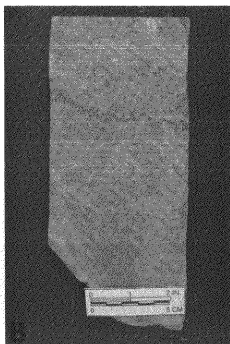
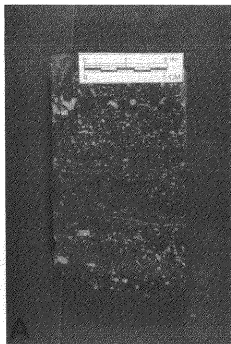




Figure 7. Core photographs of lithofacies identified from the Palo Pinto Formation.

- A. Crinoid-shale wackestone lithofacies. Principal constituents include lime mud and very fine grained terrigenous clastics. Crinoid fragments are the principal carbonate grain type. (Shell Oil Conley 7, 5214.0 ft.)
- B. Skeletal wackestone lithofacies. This lithofacies contains diverse biota with crinoids, bryozoans, and phylloid algae being the principal grain types. (Shell Oil Conley 7, 5284.0 ft.)
- C. Algal bafflestone lithofacies. This lithofacies is characterized by phylloid algae and lime mud. (Shell Oil Conley 7, 5257.0 ft.)
- D. Fusulinid-oolite packstone lithofacies. This lithofacies has a relatively high taxonomic diversity with fusulinid tests and oolites being the principal grain types. The grains are typically broken and abraded. (Sage Energy Conley 17, 5220.0 ft.)



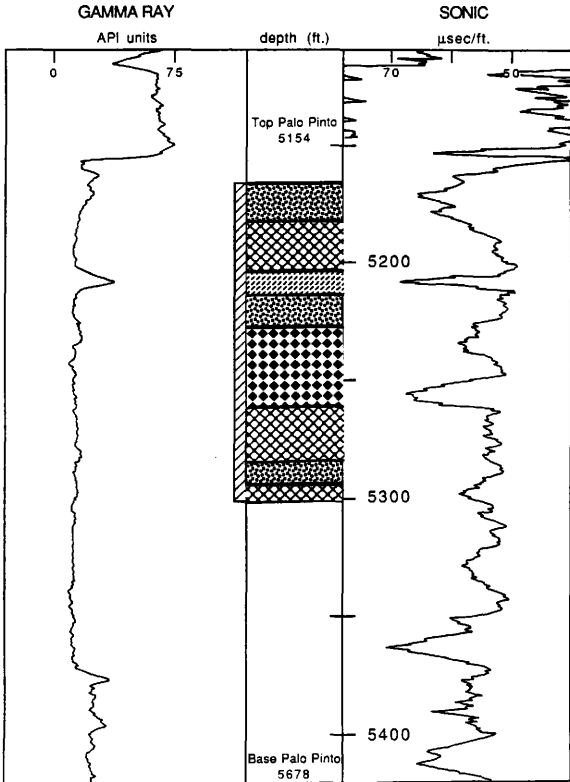
the continuous nature of the laminar structures. The lithofacies is generally less than 1 ft (0.5 m) thick except for a 4 - 12 ft (1 - 4 m) zone near the top of the cored interval. The lithofacies becomes thicker in the downdip wells. This lithofacies can be recognized by its well log character. Depending on the thickness of the unit, a large positive gamma ray deflection and large acoustic log transit time are characteristic (Figure 8). This lithofacies represents an influx of very fine grained terrigenous clastics into the center of the basin and most probably represents the typical intermound deposit between the platy algal carbonate buildups.

Skeletal wackestone lithofacies (Figure 7B). The skeletal wackestone lithofacies contains a relatively diverse biota. The principal grain types are crinoid fragments, bryozoans, phylloid algae, and miscellaneous shell fragments. Lime mud content makes up 20-70% of the rock volume. This lithofacies contains a distinctive mottled bedding which is interpreted to be the result of bioturbation. Clay laminae are present throughout the section; they exhibit wavy, subparallel, and discontinuous structures. The discontinuous nature of the laminae is a further indication of organic reworking of the sediment. The thickness of this lithofacies ranges from 20 ft (6 m) to 35 ft (11 m). The porosity in this unit is relatively low and results in a short transit time on the acoustic log (Figure





Figure 8. Well logs from the Shell Conley 7 well.  
Lithofacies patterns are defined in Figure 5. The  
cored interval from this well is indicated by the  
cross hatched section.

SHELL OIL COMPANY  
CONLEY 7

8). The lower boundary of this lithofacies is typically abrupt with the underlying crinoid-shale wackestone lithofacies. The upper boundary is gradational into the algal bafflestone or fusulinid-oolite packstone lithofacies. This lithofacies represents the initial substrate on which carbonate mounds developed.

Algal bafflestone lithofacies (Figure 7C). The algal bafflestone lithofacies is characterized by phylloid algal grains in a lime mud matrix. The algae constitute the principal grain type and increase in abundance up section within the lithofacies. The algae were presumably so successful they became the dominant grain type and precluded the presence of other organisms. Lime mud makes up approximately 60% of the total composition indicating that the algae acted as a baffle to accumulate a significant amount of fine-grained sediment. It may also have contributed to the sediment the same way Halimeda does on present-day carbonate platforms (Toomey et al, 1973). The upper boundary is abrupt and overlain by the fusulinid-oolite or skeletal wackestone lithofacies. The lower boundary is gradational with this unit preceded by the skeletal wackestone lithofacies. A feature unique to this lithofacies is the collapse breccia structure. It is interpreted to be a result of early compaction of the sediment while it was partially lithified. Algal plates do not appear to be intensely abraded or broken. The high

porosity in this lithofacies results in a comparatively long transit time on the acoustic log (Figure 8). This lithofacies is interpreted to represent an in situ accumulation of carbonate sediment and the growth of an algal reef.

Fusulinid-oolite packstone lithofacies (Figure 7D).

The fusulinid-oolite packstone lithofacies contains the least amount of lime mud and the highest taxonomic diversity. The principal grain types include foraminifera, crinoids, skeletal fragments, and intraclasts. Oolite content varies widely (0% to 90%) and can be the most common grain type. Bedding is massive over most of the lithofacies with the exception of small scale planar cross laminations in the oolitic intervals. This lithofacies is generally found in zones less than 3 ft (1 m) in thickness and is characterized by a long transit time on the acoustic log response indicating relatively high porosity (Figure 8). The lower contact of this lithofacies is abrupt with the algal bafflestone or skeletal wackestone lithofacies. The upper contact is also abrupt and may display the following features: reddish, oxidized clay laminae; intraclasts; and dissolution voids. This lithofacies is overlain by either the skeletal wackestone or crinoid-shale lithofacies and constitutes the upper unit of a sequence. The presence of oolites, intraclasts, abraded skeletal grains, and a low percentage of lime mud indicate that the fusulinid-oolite

packstone lithofacies represents the end of a shoaling upward phase of deposition.

The four lithofacies represent a model sequence for the Palo Pinto Formation. The succession of lithofacies implies a relative shallowing of the Pennsylvanian sea in the study area. The lowermost unit in the sequence is the crinoid-shale wackestone lithofacies. This lithofacies is overlain by the skeletal wackestone lithofacies. Taxonomic diversity increases upwards as terrigenous clastics decrease in abundance. The skeletal wackestone lithofacies is overlain by the algal bafflestone lithofacies, or reef facies. As the reef grew into shallower water, the muddy algal mound facies was replaced by the fusulinid-oolite packstone lithofacies, and represents the maximum sea level retreat during Palo Pinto deposition.

The first two lithofacies in a sequence (the crinoid-shale wackestone and skeletal wackestone lithofacies) are continuous and represent detrital intermound deposits. The next two lithofacies in the sequence (the algal bafflestone and fusulinid-oolite packstone lithofacies) represent deposition in progressively shallower water. As observed in the cored interval at Conley field, a sequence may not display all four lithofacies. For example, the algal bafflestone lithofacies is not present in the uppermost sequence. Three distinct sequences are present in the cored interval. The vertical section at Conley field

indicates that the succession of lithofacies studied is a series of shoaling upward sequences.

### The Reef

During the Pennsylvanian, north Texas was subjected to intense tectonic activity and the Hardeman basin existed as a shallow sea between two major uplifts. Even though coarse-grained terrigenous clastics were deposited on the northern edge of the basin (Handford, 1979), the center remained a clear-water environment. Clastic deposition in the center of the basin was limited to fine-grained silts and shales.

The algal mound at Conley field shows a carbonate accumulation of 300 - 400 ft (91 - 122 m) over the surrounding deposits (Figure 9). A paleobathymetric high has been inferred to have existed at the end of Mississippian deposition (Walters, 1984). Figure 10 shows an interval isopach of the shale unit immediately below the Palo Pinto Formation. The shale thins over the Pennsylvanian buildup indicating that a high was present at the initiation of Palo Pinto deposition.

The present structure on the Palo Pinto datum is shown in Figure 11. There is a gentle northerly dip of 5° and a present-day anticline with approximately 400 ft (122 m) of closure. A fault on the northern edge of Conley field





Figure 9. Isopach map of the Palo Pinto Formation.

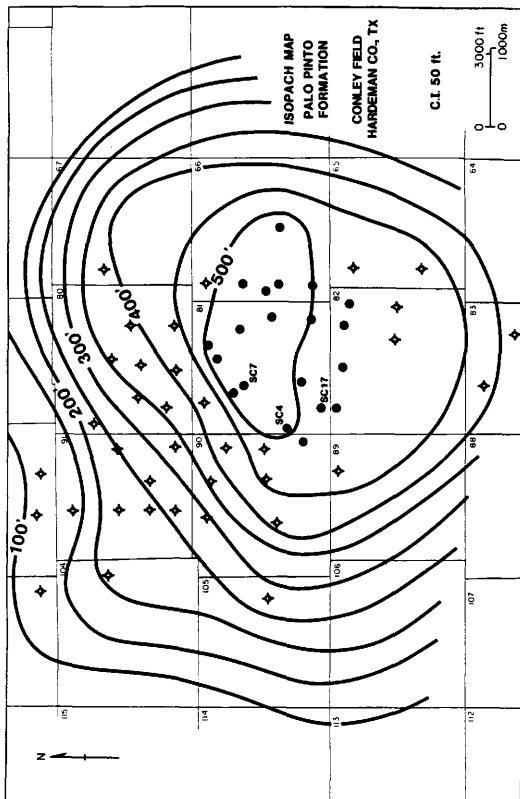




Figure 10. Interval isopach map of the shale interval underlying the Palo Pinto Formation.

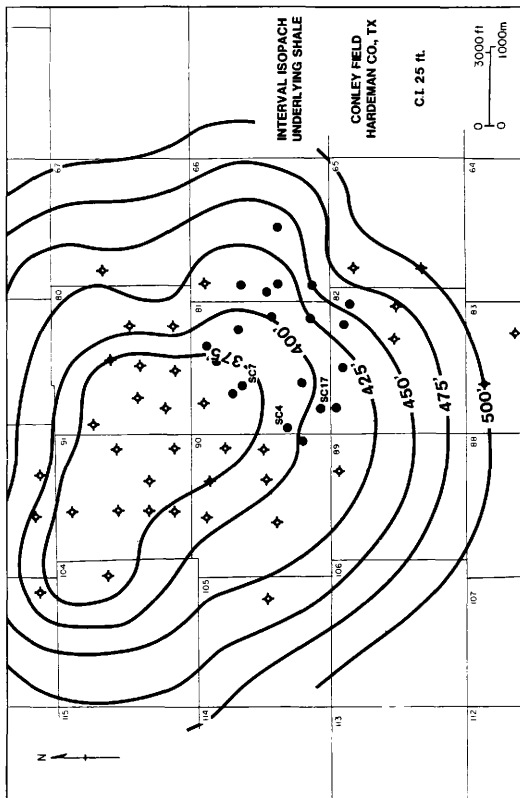
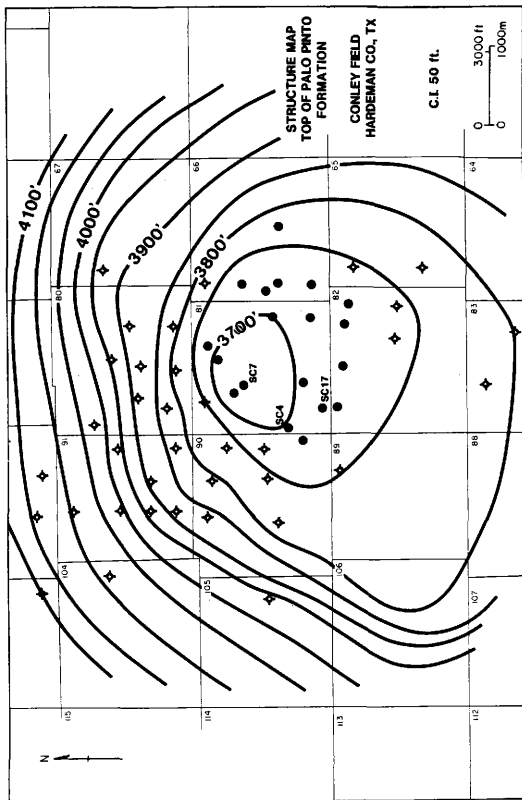




Figure 11. Present structure on top of the Palo Pinto Formation at Conley field.





(north of the map area) has approximately 100 ft (30 m) of throw and displaces Ordovician through Permian strata. This fault could be the cause of steeper dips on the north side of the field.

The distribution of lithofacies across the area is shown in Figure 12. The overall morphology of the mound is circular, with a steep side to the north and more gentle slopes to the south, east and west. The steep northern edge may be related to the basement fault mentioned above. Three of the lithofacies thin laterally and two disappear within 4000 ft (1220 m) of the mound crest (the fusulinid-oolite packstone and algal bafflestone lithofacies). The reef facies were restricted to the shallowest water areas and are not present away from the paleocrest of the mound. The detrital crinoid-shale wackestone lithofacies thickens off structure.

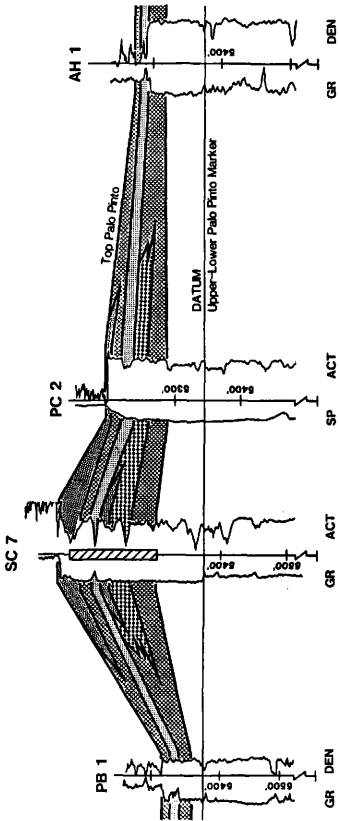
The lithofacies patterns shown on this cross section (Figure 12) reflect depositional topography present before and during growth of the algal mound. An interval isopach map of an unnamed shale unit above the Palo Pinto Formation shows thinning over the crest of the mound (Figure 13). The mound had approximately 45 ft (14 m) of relief at the end of Palo Pinto deposition with flanking beds dipping approximately  $25^{\circ}$ . Two of the lithofacies (the fusulinid-oolite packstone and algal bafflestone lithofacies) represent shallow water deposition on the paleotopographic



Figure 12. North-south stratigraphic cross section A-A' illustrating lithofacies distribution across Conley field. The location of the cross section is indicated in Figure 3. The datum is the base of the upper Palo Pinto Formation. Only facies greater than 3 feet (1 m) in thickness are shown.

SOUTH  
A'

NORTH  
A



LITHOFACIES LEGEND

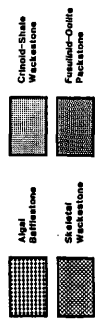
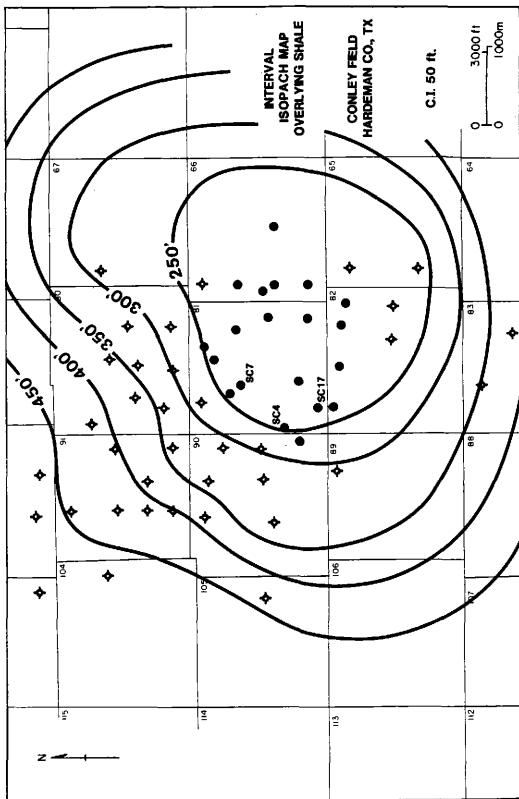




Figure 13. Interval isopach map of the shale interval overlying the Palo Pinto Formation.



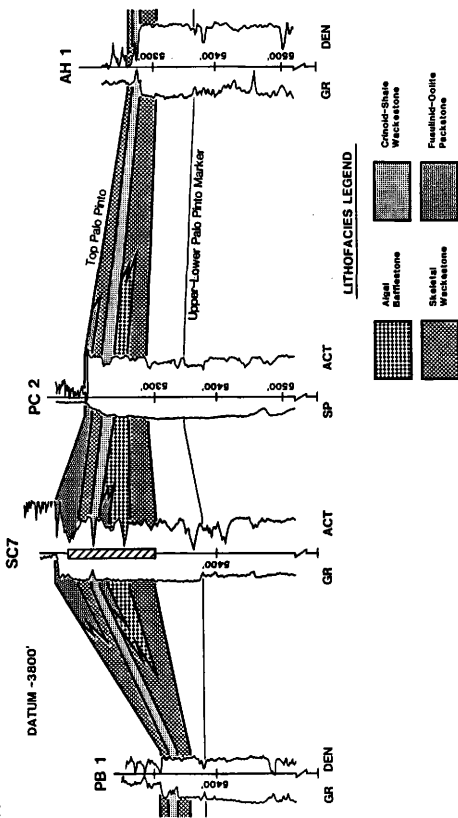
high. The other lithofacies (the crinoid-shale wackestone and skeletal wackestone lithofacies) are not as limited in bathymetric extent and represent laterally extensive, intermound deposits.

The relationship between present structure and lithofacies distribution is shown in Figure 14. The present structural crest is almost coincident with the paleotopographic crest of the mound. Structural relief has increased by approximately 100 ft (30 m) since deposition but the location of the high has remained constant since Pennsylvanian time.





Figure 14. Structural cross section A-A', illustrating lithofacies distribution and relationship to present day structure.

SOUTH  
A'NORTH  
A

## DIAGENESIS

A variety of diagenetic features are present in the Pennsylvanian rocks at Conley field. Thin section studies revealed the presence of the following features:

- 1) micritization
- 2) acicular rim cement
- 3) syntaxial overgrowths
- 4) fine to medium calcite spar
- 5) stabilization
- 6) grain breakage
- 7) dissolution
- 8) compaction
- 9) fracturing
- 10) coarse calcite spar
- 11) stylolitization
- 12) dolomitization
- 13) oil migration
- 14) sulfide mineralization

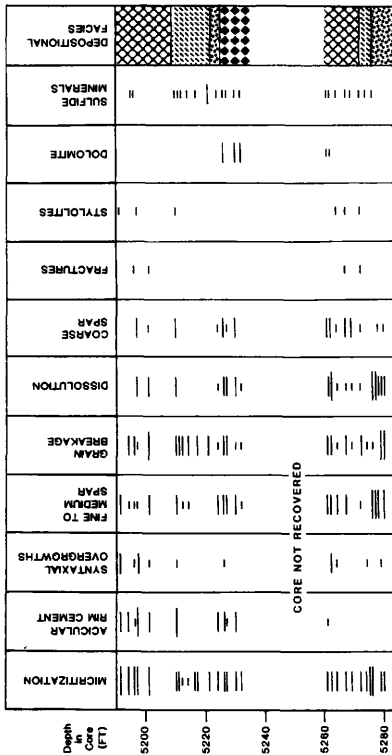
The relative abundance and distribution of these features is illustrated in Figures 15 and 16.

The process of micritization results from boring by endolithic algae or fungi in the marine environment



Figure 15. Bar graph illustrating diagenetic features identified from the Shell Conley 4 well. Lithofacies patterns are defined in Figure 5.

## SHELL CONLEY 4



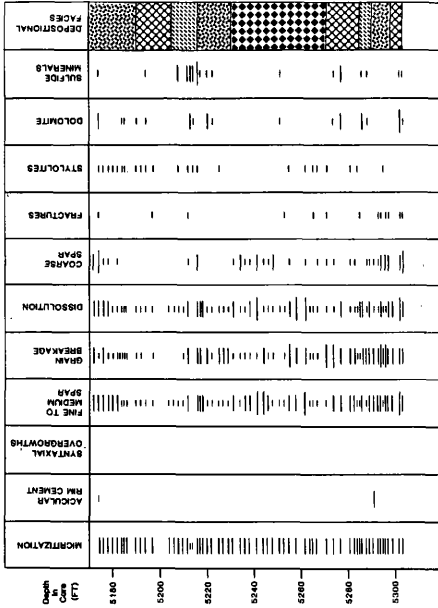
- RARE (0-10%)  
 - COMMON (20-49%)  
 - ABUNDANT (> 50%)





Figure 16. Bar graph illustrating diagenetic features identified from the Shell Conley 7 well. Lithofacies patterns are identified in Figure 5.

## SHELL CONLEY 7



- RARE (0-10%)  
 - COMMON (20-40%)  
 - ABUNDANT (> 60%)

(Bathurst, 1975). Micritization is common to abundant in the Palo Pinto rocks and is present in all four facies. The process was most extensive in the skeletal wackestone lithofacies. Elsewhere in the section, micritization was limited to grain rims and did not completely alter the internal structure of the grains.

Acicular rim cement was identified in all four facies. The cement in the Conley field rocks is presently composed of low magnesium calcite. Longman (1980) has identified similar acicular rim cements which were originally precipitated as aragonite. The cement in the Conley field rocks occurs on grain boundaries and may have been precipitated as aragonite by marine fluids. Though modern marine water is supersaturated with respect to calcium carbonate, very little cementation occurs from a single pore volume of marine water (Matthews, 1974). A large amount of water must pass through the sediment to precipitate a significant amount of cement. Tides, waves, and currents are capable of moving sufficiently large pore volumes of water (Longman, 1980). The presence of acicular rim cements on grains in Conley field rocks may indicate cementation in a relatively shallow water environment where currents and waves moved relatively large volumes of marine waters.

Syntaxial overgrowths on echinoderm fragments are rare but present at Conley field. The Palo Pinto rocks

contain overgrowths which uniformly surrounded crinoid fragments. This type of overgrowth is present, in limited amounts, in the skeletal wackestone and crinoid-shale lithofacies.

If pore waters are saturated with  $\text{CaCO}_3$ , cementation in the form of equant crystals can occur (James and Choquette, 1984). This type of cement is common in the algal bafflestone and fusulinid-oolite packstone lithofacies. It coarsens toward pore centers. This type of cementation is most common in the algal bafflestone facies where primary porosity was preserved. This equant spar occluded a portion of the primary porosity.

Aragonite and high magnesium calcite are relatively unstable in the presence of undersaturated fluids. The interaction of metastable constituents and relatively fresh pore fluids will result in the neomorphism to more stable grains and cements (Longman, 1980). This stabilization would have affected the Palo Pinto acicular rim cements and metastable skeletal grains. The diagenetic product would be the stable, low magnesium calcite seen today.

Grain breakage occurred after the precipitation of the calcite spar. This breakage is the result of loading on the sediment during early burial and continued as the sediments were more deeply buried. The most extensive breakage occurred in the fusulinid-oolite packstone and algal bafflestone lithofacies. The collapse breccia

structures in the latter facies are the result of early compaction.

The presence of moldic and vuggy porosity in the fusulinid-oolite and algal bafflestone lithofacies indicates that undersaturated water was present after deposition of the Conley Field rocks. Vuggy and moldic porosity represent dissolution in these two lithofacies (Figures 17A and 17B). Early, selective dissolution of phylloid algal grains represented by moldic porosity indicates that the algal grains may have been originally composed of aragonite or high magnesium calcite. Oomoldic porosity is present in the fusulinid-oolite packstone lithofacies. Intraparticle porosity is present in fusulinid grains and the zooecia of bryozoan fragments.

Compaction was identified by counting sutured and concavo-convex grain contacts. It is not common and occurs in the more grainy portions of lithofacies where more grain to grain contacts are present.

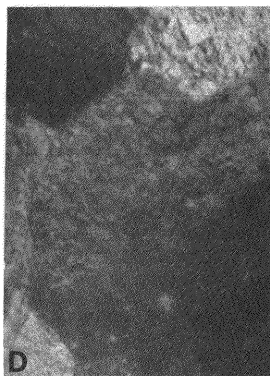
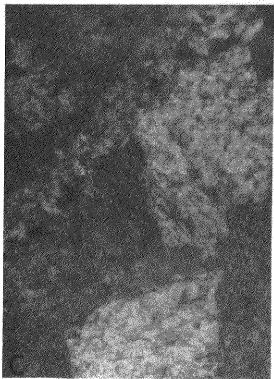
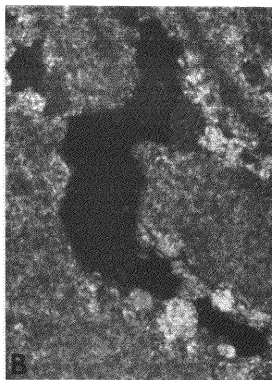
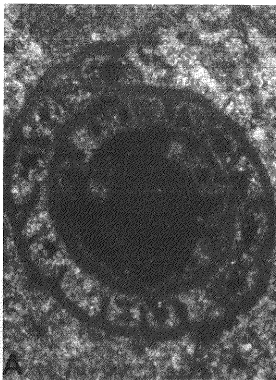
Fractures are rare in the Palo Pinto Formation at Conley Field. The fractures which are present are vertical and range up to 6 in (15 cm) in length. They truncate previous cementation events and are healed by subsequent coarsely crystalline calcite. They are most common in the skeletal wackestone and fusulinid-oolite packstone lithofacies.

Pore filling coarse calcite spar is common in the



Figure 17. Photomicrographs of diagenetic features from the Palo Pinto Formation.

- A. Dissolution in the fusulinid-oolite packstone lithofacies. Intraparticle porosity is typically located in oolites and fusulinid grains.  
(Scale: 1 in. equals 2 mm)  
(Shell Oil Conley 4, 5277.5 ft.)
  
- B. Extensive dissolution and vuggy porosity. This example is from the algal bafflestone facies and shows partial filling of the void space with blocky calcite spar.  
(Scale: 1 in. equals 2 mm)  
(Shell Oil Conley 7, 5262.0 ft.)
  
- C. Precipitation of blocky calcite spar in depositional porosity.  
(Scale: 1 in. equals 1.5 mm)  
(Shell Oil Conley 7, 5235.8 ft.)
  
- D. Late stage saddle dolomite  
(Scale: 1 in. equals 1 mm)  
(Shell Oil Conley 7, 5291.5 ft.)





fusulinid-oolite packstone and algal bafflestone lithofacies. This cement filled depositional voids and partially filled solution enlarged vugs (Figure 17C). Macroscopic crystals can be seen to have grown into the larger (>1 cm) pore spaces. The coarse cement also filled vertical fractures, indicating that it postdates the fractures.

Stylolitization is common in the Palo Pinto interval. Stylolites are most common in the skeletal wackestone lithofacies. Stylolites cut all previously mentioned diagenetic features.

Dolomite is common to rare in the Palo Pinto at Conley field. It is typically fine to medium crystalline saddle dolomite with characteristic curved crystal faces and sweeping extinction (Figure 17D). Similar dolomites have been described as late subsurface diagenetic events associated with Mississippian reservoirs elsewhere in the Hardeman basin (Ahr, 1982). Palo Pinto dolomite is commonly associated with stylolites.

Oil typically occurs in the same microspaces as the saddle dolomite. Oil was observed inside dolomite filled molds. Two stages of oil migration have been reported for Mississippian reservoirs in the Hardeman basin (Ross, 1981 and Walters, 1984); but only one episode appears to have occurred in the Palo Pinto rocks.

Pyrite is observed as a replacement mineral for

grains in the Palo Pinto rocks. The only grain which could be identified to be replaced were fusulinid tests. This type of replacement is present throughout the interval and appears to cut all previous diagenetic events.

## THE RESERVOIR

The Palo Pinto reservoir at Conley field produces oil from the upper 100 ft (30 m) of the formation. Tables 2 and 3 show reservoir properties and production statistics for the productive Palo Pinto interval.

Average porosity and permeability for the four lithofacies are as follows: fusulinid-oolite packstone - 9%, 2.0 md; algal bafflestone - 8%, 0.6 md; skeletal wackestone - 4%, 0.5 md; and crinoid-shale wackestone - less than 3%, less than 0.1 md. Production is limited to the more porous and permeable fusulinid-oolite packstone and algal bafflestone lithofacies. The relationships between porosity, permeability, fluid saturations, and lithofacies in the Shell Conley 7 core are shown in Figure 18. A fault to the north of the field has caused an increase in the dip of the productive interval but does not affect Pennsylvanian oil and gas production.

Depositional porosity existed initially in the high grain:mud ratio rocks, especially in the algal mound core where pores were present as shelter voids. The depositional porosity was greatly reduced by calcite spar cementation. Dissolution by undersaturated fluids created: 1) moldic porosity of algal plates in the algal bafflestone lithofacies; 2) intraparticle porosity of fusulinids, oolites, and bryozoans in the fusulinid-oolite packstone

Table 2. Summary of initial reservoir properties for the productive Palo Pinto interval at Conley field. Information obtained from Railroad Commission of Texas field files.

---

Original Pressure	2309 psig
Original Volume Factor	1.188 at saturation pressure
Average Reservoir Temp.	146° F
Average Oil Gravity	41° API
Average Producing GOR	395 cf/b
Salinity of Water	140,000 ppm Cl <sup>-</sup>
Average Porosity	8%
Average Permeability	3.3 md
Water Saturation	30%
Type of Drive	Water
Estimated Orig. Oil in Place	1,140,000+ bbls
Accumulative Production (1-1-87)	1,552,306 bbls
Depth of Oil-Water Contact	-3785 ft
Average Depth Top of Pay	5180 ft (-3715 ft)
Average Net Pay	13 ft
Average Dip Producing Zone	125 ft/mile

Table 3. Production history for Conley (Palo Pinto) field, Hardeman County, Texas. Data includes production from the Palo Pinto Formation to January 1, 1987. Information obtained from Railroad Commission of Texas Annual Reports (1960-1986).

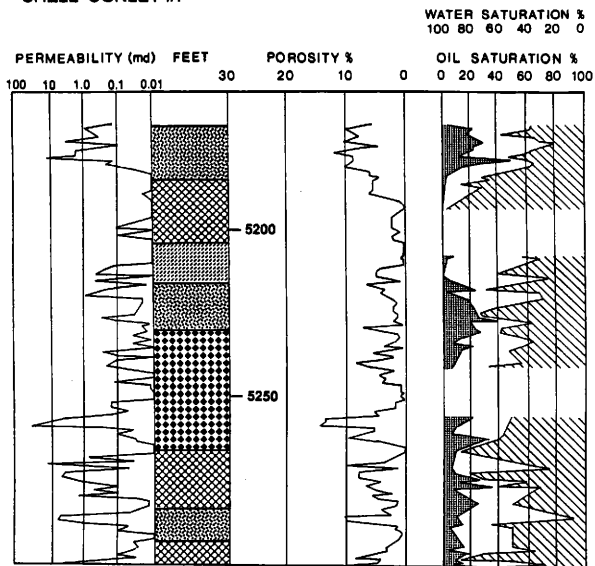
Year	Casinghead gas* (MCF)	Crude Oil (BBLs)	Accumulative Crude Oil (BBLs)
1960		18,459	18,459
1961		101,828	120,287
1962		83,128	203,415
1963		112,400	315,815
1964		160,582	476,397
1965		152,958	629,355
1966		144,317	773,672
1967	35,611	113,498	887,170
1968	28,044	101,171	988,341
1969	24,650	75,726	1,064,067
1970	32,679	65,046	1,129,038
1971	31,362	54,998	1,184,036
1972	21,718	49,682	1,233,718
1973	18,706	44,318	1,278,036
1974	18,910	36,949	1,314,985
1975	16,417	34,484	1,349,469
1976	13,126	23,714	1,373,183
1977	12,086	21,905	1,395,088
1978	9533	21,201	1,416,289
1979	8881	20,825	1,435,211
1980	7185	19,699	1,454,910
1981	6256	17,615	1,472,525
1982	6019	15,784	1,488,309
1983	4293	17,346	1,505,655
1984	2737	14,745	1,520,522
1985	4075	15,313	1,535,835
1986	5560	16,471	1,552,306

\* For the years 1960-66, casinghead gas was reported with crude oil production.



Figure 18. Relationship between porosity, permeability, fluid saturations, and lithofacies from the Shell Conley 7 well. Cored interval is 5170.0 - 5304.1 ft.

## SHELL CONLEY #7



## LITHOFACIES LEGEND



Algal Bafflestone



Crinoid-Shale Wackestone



Skeletal Wackestone



Fusulinid-Oolite Packstone



lithofacies; and 3) vuggy porosity present in both these lithofacies. A partial reduction in porosity was caused by compaction of the sediment during burial and cementation by coarse calcite spar. This reduction did not, however, completely occlude all pore space in the rock.

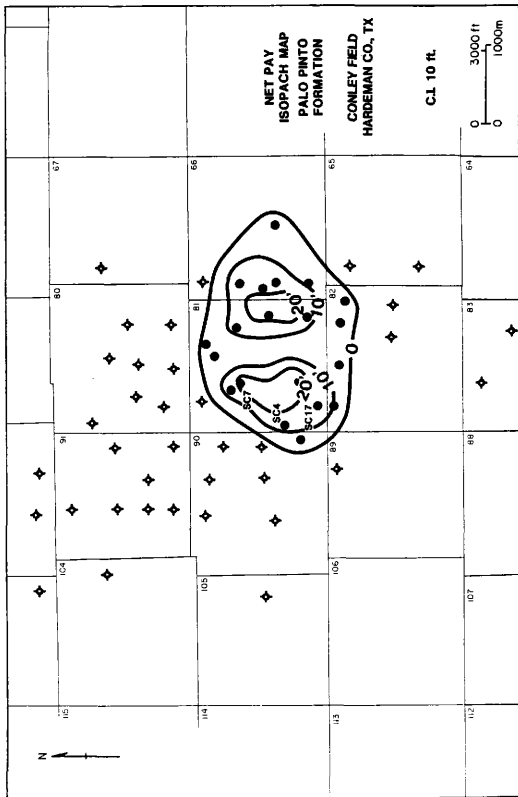
The amount of porosity varies laterally across the field. Vuggy porosity was most extensive in the updip well (Shell Conley 7). This well was structurally high during deposition of the Palo Pinto sediments.

Porosity at Conley field is the result of the interaction of depositional and diagenetic events. Porosity is highest in the grainiest facies. Preserved primary porosity was enlarged through dissolution by undersaturated fluids. The location of dissolution porosity is on the crest of the paleotopographic high. Since present day structure is coincident with the paleotopographic high, the highest porosity values at Conley field are located on the present day structural crest. A net pay isopach map of the productive Palo Pinto interval at Conley field indicates that the productive interval is coincident with the crest of the paleotopographic high (Figure 19).

In order to understand the distribution of reservoir porosity in fields similar to Conley field, a thorough study of the depositional history is necessary with special emphasis placed on paleotopography and early diagenesis. Exploration and exploitation of reservoirs similar to this



Figure 19. Net pay isopach map of the productive Palo Pinto Formation.



one should focus on locating depositional thicks associated with paleotopographic highs of pre-palo Pinto age.

Diagenesis acted to increase porosity in the grainiest facies on the crests of paleohighs.

## CONCLUSIONS

The carbonate rocks comprising the Palo Pinto Formation at Conley field are the result of an interaction of depositional and diagenetic events. The following conclusions were reached by this study:

The upper Palo Pinto Formation at Conley field is a series of carbonate deposits representing the growth of a phylloid algal reef. A succession of lithofacies defines a standard sequence for the Palo Pinto Formation and represents a relative shallowing of the Pennsylvanian sea in the study area. The buildup was localized on a pre-Pennsylvanian high with the present structural crest almost coincident with the paleotopographic crest of the reef.

Porosity in the upper Palo Pinto Formation is the result of depositional and subsequent diagenetic processes. The highest porosity is in the grainiest facies; however, only a portion of the primary porosity was preserved. Early stage dissolution by undersaturated pore fluids greatly increased porosity. The location of the diagenetic enhanced porosity was controlled by facies locations and topography present during deposition of the algal

mound. The most extensive dissolution and consequently the largest porosity, is located in the grainiest facies at paleostructural highs.

## REFERENCES CITED

- Ahr, W.M., 1982, Saddle crystal dolomites as fractured reservoir indicators, Mississippian biohermal facies, Hardeman County, Texas: Gulf Coast Association of Geological Societies, Transactions, vol. 32, p.195-198.
- Ahr, W.M. and S.L. Ross, 1982, Chappel (Mississippian) biohermal reservoirs in the Hardeman Basin, Texas: Gulf Coast Association of Geological Societies, Transactions, vol. 32, p.185-193.
- Allison, M.D., 1979, Petrology and depositional environments of the Mississippian Chappel bioherms, Hardeman County, Texas: unpublished M.S. Thesis, West Texas State University, 53p.
- Bathurst, R.G.C., 1975, Carbonate sediments and their diagenesis: Elsevier Scientific Publishing Co., New York, 658p.
- Budnik, R.T., 1983, Recurrent motion on Precambrian-age basement faults, Palo Duro Basin, Texas panhandle: abstract, American Association of Petroleum Geologists, Bulletin, vol. 67, no. 3, p.433.
- Campbell, C.V., 1967, Lamina, laminaset, bed and bedset: Sedimentology, vol. 8, no. 1, p.7-26.
- Choquette, P.W., 1983, Platy algal reef mounds, Paradox Basin: in P.A. Scholle, D.G. Bebout, and C.H. Moore, eds., Carbonate depositional environments: American Association of Petroleum Geologists, Memoir 33, p.454-462.
- Choquette, P.W. and L.C. Pray, 1970, Geologic nomenclature and classification of porosity in sedimentary carbonates: American Association of Petroleum Geologists, Bulletin, vol. 54, no. 2, p.207-250.
- Choquette, P.W. and J.D. Trout, 1963, Pennsylvanian carbonate reservoirs, Ismay Field, Utah and Colorado: in R.O. Bass and S.L. Sharps, eds., Shelf carbonates of the Paradox Basin, a symposium: Four Corners Geological Society, Fourth Field Conference, p.157-184.
- Cummins, W.F., 1891, Report on the geology of northwestern Texas, part II, economic geology: in E.T. Dumble, ed., Second annual report of the Geological Survey of Texas: Texas Geological Survey, Annual Report, p.359-555.



- Dunham, R.J., 1969, Early vadose silt in Townsend Mound (reef) New Mexico: *in* G.M. Friedman, ed., Depositional environments in carbonate rocks: Society of Economic Paleontologists and Mineralogists, Special Publication, no. 14, p.139-181.
- Dunham, R.J., 1962, Classification of carbonate rocks according to depositional texture: *in* W.E. Ham, ed., Classification of carbonate rocks - a symposium: American Association of Petroleum Geologists, Memoir 1, p.108-121.
- Embry, A.F. and J.E. Klovan, 1971, A late Devonian reef tract on northeastern Banks island, N.W.T.: Canadian Petroleum Geology, Bulletin, vol. 19, p.730-781.
- Erxleben, A.W., 1975, Depositional systems in Canyon Group (Pennsylvanian System), north-central Texas: Bureau of Economic Geology The University of Texas, Report of Investigations, no. 82, 76p.
- Flawn, P.T., 1956, Basement: not the bottom but the beginning: American Association of Petroleum Geologists, vol. 49, no. 7, p.833-886.
- Flugel, E., 1978, Microfacies analysis of limestones: Springer-Verlag, New York, 633p.
- Freeman, J.C., 1964, The Conley Field, Hardeman County, Texas: Tulsa Geological Society, Digest, vol. 32, p.126-130.
- Goldstein, A.G. and D.A. McGookey, 1982, Minor fault motions in relationship to late Paleozoic tectonics of the Wichita Uplift: abstract, Geological Society of America, Abstracts with Programs, vol. 14, no. 3, p.111-112.
- Handford, C.R., 1979, Depositional and diagenetic history of high-constructive delta systems (Wolfcampian), southeastern Palo Duro Basin, Texas: *in* N.J. Hyne, ed., Pennsylvanian sandstones of the mid-continent, Tulsa Geological Society, p.247-259.
- Herrod, W.H., M.H. Roylance, and E.C. Strathouse, 1985, Pennsylvanian phylloid algal mound production at Tin Cup Mesa Field, Paradoz Basin, Utah: *in* M.W. Longman, K.W. Lindsay, and D.E. Eby, eds., Rocky Mountain carbonate reservoirs - a core workshop: Society of Economic Paleontologists and Mineralogists, Core Workshop No. 7, p.409-445.

- James, N.P., 1983, Reef environment: in P.A. Scholle, D.G. Bebout, and C.H. Moore, eds., Carbonate depositional environments: American Association of Petroleum Geologists, Memoir 33, p.345-440.
- James, N.P. and P.W. Choquette, 1984, The meteoric diagenetic environment: Geoscience Canada, vol. 11, no. 4, p.161-194.
- Keller, G.R. and S.E. Cebull, 1973, Plate tectonics and the Quachita System in Texas, Oklahoma, and Arkansas: Geological Society of America, Bulletin, vol. 84, no. 5, p.1659-1666.
- Kerr, S.D., Jr., 1969, Algal-bearing carbonate reservoirs of Pennsylvanian age, west Texas and New Mexico: abstract, American Association of Petroleum Geologists, Bulletin, vol. 53, no. 3, p.726-727.
- King, P.B., 1975, Ancient southern margin of America: Geology, vol. 3, no. 12, p.732-734.
- Longman, M.W., 1980, Carbonate diagenetic textures from nearsurface diagenetic environments: American Association of Petroleum Geologists, Bulletin, vol. 64, no. 4, p.461-487.
- Matthews, R.K., 1974, A process approach to diagenesis of reefs and reef associated limestones: in L.F. Laporte, ed., Reefs in time and space: Society of Economic Paleontologists and Mineralogists, Special Publication Number 18, p.234-256.
- Montgomery, S.L., 1984, Hardeman Basin -- small, oil-rich graben in north Texas: Petroleum Information, Petroleum Frontiers, vol. 1, no. 2, 68p.
- Oil and Gas Journal, 1961, Conley promises action in Texas: vol. 59, no. 17, p.215-216.
- Peterson, J.A., 1959, Petroleum geology of the Four Corners area: Proceedings, Fifth World Petroleum Congress, Sec. 1, Paper 27, p.499-523.
- Pray, L.C. and J.L. Wray, 1963, Porous algal facies (Pennsylvanian), Honaker Trail, San Juan Canyon, Utah: in R.O. Bass and S.L. Sharps, eds., Shelf carbonates of the Paradox Basin, a symposium: Four Corners Geological Society, Fourth Field Conference, p.204-234.
- Railroad Commission of Texas, 1960-1986, Annual report: Oil and Gas Division, Austin.

- Ross, S.L., 1981, Origin and diagenesis of Mississippian carbonate buildups, Quanah Field, Hardeman County, Texas: unpublished M.S. Thesis, Texas A&M University, 142p.
- Ruppel, S.C., 1984, The Chappel Formation (Mississippian) of the eastern Palo Duro Basin: development of a carbonate shoal: in P.M. Harris, ed., Carbonate sands - a core workshop: Society of Economic Paleontologists and Mineralogists, Core Workshop No. 5, p.58-93.
- Schatzinger, R.A., 1983, Phylloid algal and sponge-bryozoan mound-to-basin transition: a late Paleozoic facies tract from the Kelly-Snyder Field, west Texas: in P.M. Harris, ed., Carbonate buildups - a core workshop: Society of Economic Paleontologists and Mineralogists, Core Workshop No. 4, p.244-303.
- Schlumberger, 1987, Log interpretation principles / applications: Schlumberger Educational Services, Houston, 198p.
- Shinn, E.A., D.M. Robbin, B.H. Lidz, and J.H. Hudson, 1983, Influence of deposition in two Paleozoic buildups: Mississippian and Permian age rocks in the Sacramento Mountains, New Mexico: in P.M. Harris, ed., Carbonate buildups - a core workshop: Society of Economic Paleontologists and Mineralogists, Core Workshop No. 4, p.182-222.
- Soderstrom, G.S., 1968, Stratigraphic relationships in the Palo Duro - Hardeman Basin area: in , Basins of the Southwest: American Association of Petroleum Geologists, Symposium at 10th Annual Meeting Southwest Section, vol. 1, p.41-49.
- Tarr, R.S., 1890, Preliminary report on the coal fields of the Colorado River: in E.T. Dumble, ed., First annual report of the Geological Survey of Texas: Texas Geological Survey, Annual Report, p.201-216.
- Thomas, W.A., 1985, The Appalachian-Quachita connection: Paleozoic orogenic belt at the southern margin of North America: in , Annual Review of Earth and Planetary Sciences: Annual Reviews, Inc., vol. 13, p.175-199.
- Toomey, D.F., J.L. Wilson, and R. Rezak, 1977, Evolution of Yucca mound complex, late Paleozoic phylloid-algal buildup, Sacramento Mountains, New Mexico: American Association of Petroleum Geologists, Bulletin, vol. 61, no. 12, 2115-2133.

- Toomey, D.F. and H.D. Winland, 1973, Rock and biotic facies associated with middle Pennsylvanian (Desmoninesian) algal buildup, Nena Lucia Field, Nolan County, Texas: American Association of Petroleum Geologists, Bulletin, vol. 57, no. 6, p.1053-1074.
- Walper, J.L., 1977, Paleozoic tectonics of the southern margin of North America: Gulf Coast Association of Geological Societies, Transactions, vol. 27, p.230-241.
- Walters, J.K., 1984, The depositional and diagenetic history of the Chappel Formation, Conley Field, Hardeman County, Texas: unpublished M.S. Thesis, Texas A&M University, 125p.
- Wilson, J.L., 1975, Carbonate facies in geologic history: Springer-Verlag, New York, 471p.

APPENDIX A  
WELL DATA BASE

W & RR Survey Block H Section	Operator	Fee Name	DF (ft)	TD (ft)	Palo Pinto	
					Top (ft)	Thickness (ft)
64	Pan American	Hamilton 1	1487	8660	5294	392
65	Phillips	Lockhart A-1	1460	8201	5205	485
	Phillips	Lockhart A-2	1467	8215	5222	470
	Shell Oil & Pan American	Cascade 1	1467	8257	5198	493
66	Shell Oil	Melear 1	1468	8418	5236	492
	Shell Oil	Melear A-1	1465	8236	5181	504
	Shell Oil	Melear 2	1468.5	8229	5188	505
	Shell Oil	Melear 2A	1454	8223	5168	502
	Shell Oil	Melear 3A	1460	8215	5222	504
	Shell Oil	Melear 4A	1468	5234	5177	---
67	United Prod.	Welch 1	1486	8504	5401	398
80	Pure Oil	Tabor 1	1471	8251	5280	440
	Shell Oil	Flynn 1	1477	8270	5321	379
	Shell Oil	Flynn A-1	1494	8307	5522	243
	Shell Oil	Flynn 3	1485	8238	5378	348
	Shell Oil	Self 1	1482	8241	5275	420
	Shell Oil	Self 2	1482	8244	5375	365
	Shell Oil	Self 3	1487	8243	5440	375
	Shell Oil	Tabor 1	1483	8245	5370	392
81	Amerada	Rice 1	1476	8255	5162	523
	Sage Energy	Conley 17	1468	8234	5182	496
	Shell Oil	Conley 1	1481	8577	5197	503
	Shell Oil	Conley 4	1466	8097	5174	502

W & RR Survey Block H			Palo Pinto			
Section	Operator	Fee Name	DF (ft)	TD (ft)	Top (ft)	Thickness (ft)
81	Shell Oil	Conley 5	1471	9310	5240	418
	Shell Oil	Conley 6	1462	8223	5183	491
	Shell Oil	Conley 7	1474	8334	5154	524
	Shell Oil	Conley 8	1479	8242	5173	522
	Shell Oil	Conley 9	1460	8209	5175	503
	Shell Oil	Conley 12	1470	8234	5175	520
	Shell Oil	Conley 14	1468	8220	5170	520
82	Phillips	Conley A-1	1472	8285	5205	485
	Phillips	Conley A-2	1474	8238	5198	494
	Phillips	Conley A-3	1470	8212	5195	493
	Phillips	Conley A-4	1471	8212	5195	492
	Phillips	Conley A-5	1455	8196	5192	486
	Phillips	Conley A-6	1472	8215	5198	482
83	Apache Explor.	Holmes 1	1489	8305	5288	428
	Westheimer- Neustadt	Holmes 1	1475	8502	5262	432
89	Shell Oil	Conley B-1	1483	8346	5225	473
90	Shell Oil	Conley A-1	1470	8227	5292	428
	Shell Oil	Conley A-2	1476	8229	5315	365
	Shell Oil	Conley D-1	1485	8242	5378	297
	Shell Oil	Irvin 1	1485	8242	5268	432
	Shell Oil	Wilson 1	1478	9469	5200	485
	Shell Oil	Wilson 3	1465	8225	5188	487

W & RR Survey Block H			Palo Pinto			
Section	Operator	Fee Name	DF (ft)	TD (ft)	Top (ft)	Thickness (ft)
90	Shell Oil	Wilson 4	1470	8241	5232	483
91	Paul DeCleva	Berngen 1	1480 (approx.)	8198	5318	258
	Pure Oil	Berngen 1	1479	8249	5305	314
	Shell Oil	Berngen 1	1483	8240	5340	320
	Shell Oil	Berngen 2	1487	8240	5418	231
	Shell Oil	Lamberton 1	1491	8253	5480	260
	Shell Oil	Schur 1	1491	8257	5495	215
	Shell Oil	Schur 2	1498	8256	5605	133
92	Shell Oil	Davis 1	1508	9457	5620	130
	Shell Oil	Davis 2	1519.6	8274	5640	113
103	Rhodes Drilling	McNabb 1	1510	8521	5715	105
104	Kimbell and Swick	Irvin 1	1506	8394	5580	205
105	Argonaut Energy & Shell Oil	West Texas Utilities 201	1490	8299	5455	290



APPENDIX B  
CORE DESCRIPTIONS  
AND  
PETROGRAPHIC DATA

## CORE DESCRIPTION

WELL: Shell Oil Company, Conley 7 (Section 81)  
 FIELD: Conley Field, Hardeman County, Texas  
 FORMATION: Palo Pinto Formation, Canyon Group: Upper  
 Pennsylvanian  
 DEPTH: 5170.0 - 5304.2 feet

DEPTH (feet)	INTERVAL (feet)	DESCRIPTION
5170.0	0.8	Limestone; wackestone; dark gray; medium grained; high taxonomic diversity; abraded misc. skeletal and fusulinid grains; stylolites.
5170.8	1.2	Limestone; packstone; dark gray; fine to medium grained; bioturbated; abraded misc. skeletal and algal grains; calcite spar replacing some grains.
5172.0	1.0	MISSING SECTION
5173.0	1.6	Limestone; packstone; dark brown; fine to medium grained; bioturbated; phylloid algae and misc. skeletal grains; calcite crystals filling vugs; oil stain.
5174.6	7.7	Limestone; wackestone; dark brown to gray; fine grained; bioturbated; misc. skeletal, fusulinid, and phylloid algal grains; stylolites; spar replacing grains; slight oil stain.
5182.3	2.8	Limestone; packstone; dark brown to gray; fine to medium grained; abraded misc. skeletal and fusulinid grains; stylolites clay lamina (1.5 cm wide).

DEPTH (feet)	INTERVAL (feet)	DESCRIPTION
5185.1	4.9	Limestone; wackestone; dark gray; fine grained; mottled bedding; misc. skeletal and phylloid algal grains; stylolites; clay laminae (wavy, nonparallel, discontinuous).
5190.0	2.0	Limestone; mudstone; gray; fine grained; phylloid algal grains; clay laminae (wavy, nonparallel, discontinuous).
5192.0	5.0	Limestone; wackestone; gray; fine grained; mottled bedding; phylloid algal, crinoid, and misc. skeletal grains; numerous stylolites.
5197.0	5.0	MISSING SECTION
5202.0	7.2	Limestone; alternating mudstone and wackestone; dark gray; fine grained; phylloid algal and crinoid grains; clay laminae (wavy, nonparallel, discontinuous); less stylolites than above section.
5209.2	3.8	Shaly limestone; wackestone; greenish gray; crinoid columnals concentrated along clay laminae; clay laminae (wavy, nonparallel, continuous).
5213.0	3.1	Limy shale; dark green to black; very fine grained; crinoid grains; wispy bedding.
5216.1	3.9	Limestone; wackestone; tan to brown; fine to medium grained; misc. skeletal, algal, and fusulinid grains; numerous stylolites, calcite crystals in vugs; slight oil stain.

DEPTH (feet)	INTERVAL (feet)	DESCRIPTION
5220.0	6.0	Limestone; wackestone to mudstone; gray; fine grained; misc. skeletal and fusulinid grains; numerous stylolites; calcite crystals in vugs; vugs approx. 1 cm in diameter.
5226.0	3.8	Limestone; wackestone; gray to brown; fine grained; phylloid algal, fusulinid, and misc. skeletal grains; algal layering; stylolites; slight oil stain.
5229.8	24.2	Limestone; wackestone; gray to brown; fine grained; predominantly phylloid agial grains; other grains include bryozoans and crinoids; calcite filled vugs; few laminae (wavy, nonparallel, discontinuous); stylolites; slight oil stain at top of section.
5254.0	9.2	Limestone; bafflestone; light gray to tan; medium grained; exclusively phylloid algal grains; numerous calcite filled vugs; collapse breccia; oil stain in vugs and associated with algal grains.
5263.2	19.6	Limestone; wackestone; gray to tan; fine grained; poorly sorted; bioturbated; misc. skeletal, phylloid algal, and bryozoan grains; stylolites; few vugs; clay laminae (wavy, nonparallel, continuous).
5282.8	1.2	Limestone; packstone; gray; medium grained; high taxonomic diversity; misc. skeletal and phylloid algal grains; stylolites, vuggy porosity.

DEPTH (feet)	INTERVAL (feet)	DESCRIPTION
5284.0	4.2	Limestone; wackestone; gray; fine grained; bioturbated; misc. skeletal grains; >3 cm section of clay laminae (inclined, parallel, continuous).
5288.2	1.8	Limestone; packstone; gray; medium grained; phylloid algal and crinoid grains; large mollusc (?) grain (> 2 cm); stylolites.
5290.0	3.8	Limestone; wackestone; dark to light gray; fine grained; phylloid algal and misc. skeletal grains; bryozoan encrusting crinoid grain; numerous stylolites; fractures filled with calcite spar; vuggy porosity (2 cm maximum diameter).
5293.8	4.2	Limestone; packstone to wackestone; gray; medium to fine grained; bioturbated; misc. skeletal and phylloid algal grains; intraclasts; stylolites.
5298.0	6.2	Limestone; wackestone; gray; fine grained; mottled bedding; misc. skeletal, phylloid algal, and coral grains; 15 cm interval of intraclasts; clay laminae (inclined, parallel, continuous); few stylolites; vugs without calcite spar filling.
5304.2		END OF CORE

PETROGRAPHIC ANALYSIS  
 Shell Oil Conley 7  
 Conley Field  
 Hardeman County, Texas  
 Palo Pinto Formation

Depth ft	mol %	bra %	for %	pa %	bry %	cri %	int %	oo %	sil %	lm %	pel %	cem %	unk %
5171.5	33	0	7	5	8	12	0	0	0	19	5	11	0
5174.0	8	0	12	16	20	19	0	0	0	15	0	10	0
5176.3	12	3	10	5	8	17	0	0	0	41	0	4	0
5177.8	10	2	4	6	5	8	0	0	0	53	10	2	0
5180.2	7	3	5	25	18	10	5	0	0	22	3	2	0
5181.5	4	2	2	42	6	8	0	0	0	36	0	0	0
5183.5	15	3	12	10	8	7	0	0	0	37	6	2	0
5184.9	4	2	4	7	10	15	0	0	0	44	13	1	0
5186.3	5	5	3	12	5	10	12	0	0	38	0	0	10
5189.5	5	3	0	16	4	6	0	0	0	53	10	3	0
5191.7	5	2	0	9	3	6	0	0	0	67	8	0	0
5193.7	3	2	0	10	17	3	0	0	0	56	9	0	0
5196.6	5	5	0	16	0	3	0	0	0	38	32	0	1
5204.0	5	2	2	10	5	4	0	0	0	41	30	0	1
5205.5	0	0	0	6	9	11	0	0	0	49	24	0	1
5208.3	2	3	0	2	10	14	0	0	0	48	20	0	1
5209.9	4	2	0	4	11	10	19	0	0	39	11	0	0
5211.5	0	0	0	9	6	5	21	0	4	46	9	0	0
5216.0	8	12	8	0	7	12	18	0	0	29	0	0	6
5218.0	2	0	5	23	5	2	0	0	0	59	0	0	4
5219.5	9	6	27	13	10	5	17	0	0	8	5	0	0
5221.5	0	0	7	0	3	2	24	0	0	61	0	0	3
5224.8	3	2	16	9	5	5	22	0	0	13	21	0	4
5226.7	0	0	21	5	1	3	31	0	0	20	19	0	0
5228.8	3	2	18	15	3	2	37	0	0	14	6	0	0
5230.5	2	2	1	24	6	8	0	0	0	57	0	0	0
5234.0	3	2	0	17	0	3	0	0	0	52	0	23	0
5235.8	1	3	12	21	3	6	0	0	0	41	4	9	0
5237.8	5	3	5	32	1	4	0	0	0	40	5	5	0
5240.5	0	5	11	19	5	2	0	0	0	23	8	27	0
5243.7	3	7	4	21	0	0	9	0	0	11	6	39	0
5246.0	3	2	0	31	4	5	2	0	0	29	4	20	0
5248.0	5	3	5	8	12	16	4	0	0	37	4	6	0
5250.5	13	7	2	18	12	5	0	0	0	38	0	2	3
5253.2	5	3	2	15	5	2	13	0	0	42	8	5	0
5255.0	0	0	0	27	5	3	0	0	0	53	0	12	0
5258.0	0	0	0	11	4	0	30	0	0	35	13	7	0
5262.0	0	0	0	21	0	0	0	0	0	59	0	8	12
5263.8	0	0	0	23	0	0	10	0	0	47	10	2	8

## PETROGRAPHIC ANALYSIS

Shell Oil Conley 7

Conley Field

Hardeman County, Texas

Palo Pinto Formation

Depth ft	mol %	bra %	for %	pa %	bry %	cri %	int %	oo %	sil %	lm %	pel %	cem %	unk %
5265.4	11	4	22	8	0	0	0	0	0	37	13	0	5
5267.0	3	2	7	8	4	6	0	0	0	41	14	6	9
5271.4	4	1	7	3	0	5	0	0	0	19	41	20	0
5274.2	6	4	3	7	6	9	0	0	0	10	25	30	0
5276.8	5	0	0	4	6	5	0	0	0	23	20	37	0
5281.0	5	2	0	6	0	4	0	0	0	33	18	32	0
5283.0	3	0	0	12	7	8	0	0	0	24	10	36	0
5283.8	11	11	5	13	0	8	0	0	0	22	19	0	11
5284.5	4	6	0	11	4	5	0	0	0	30	22	18	0
5285.8	0	0	0	0	21	24	0	0	46	9	0	0	0
5287.7	5	15	13	12	0	0	9	0	0	16	8	22	0
5289.0	3	2	9	16	0	11	4	0	0	8	17	30	0
5290.6	2	3	0	10	5	10	6	0	0	19	9	36	0
5292.8	5	0	7	8	5	10	0	0	0	14	11	40	0
5293.7	5	3	22	11	5	4	5	0	0	9	6	30	0
5294.8	5	9	3	0	3	9	16	0	0	20	11	24	0
5295.8	0	0	0	4	3	3	5	0	0	42	18	21	4
5297.3	9	11	0	5	3	4	0	0	0	33	11	24	0
5299.0	4	2	2	5	2	4	0	0	0	21	22	38	0
5301.5	0	4	0	0	0	0	0	0	0	18	17	61	0
5303.0	5	2	0	7	3	5	0	0	0	18	22	38	0

## CORE DESCRIPTION

WELL: Shell Oil Company, Conley 4 (Section 81)  
 FIELD: Conley Field, Hardeman County, Texas  
 FORMATION: Palo Pinto Formation, Canyon Group: Upper  
 Pennsylvanian  
 DEPTH: 5190.0 - 5280.0 feet

DEPTH (feet)	INTERVAL (feet)	DESCRIPTION
5190.0	5.1	Limestone; wackestone; light gray; fine grained; mottled bedding; misc. skeletal grains; clay laminae (wavy, nonparallel, continuous); stylolites.
5195.1	1.8	Limestone; packstone; light gray; fine grained; misc. skeletal, crinoid, and bryozoan grains; stylolite.
5196.9	7.1	Limestone; wackestone; dark to light gray; fine grained; bioturbated; misc. skeletal and crinoid grains; clay laminae (wavy, nonparallel, continuous), few stylolites.
5204.0	5.0	MISSING SECTION
5209.0	0.8	Limestone; packstone; dark gray; fine grained; misc. skeletal and crinoid grains; becoming more shaly down section.
5210.0	12.0	Limy shale; greenish gray to black; very fine grained; occasional limestone stringers < 10 cm thick; clay laminae (wavy, parallel, continuous); crinoid and bryozoan grains; crinoid columnals concentrated along clay laminae; "poker-chip" breakage in certain intervals; some pyrite replacement near base of section.



DEPTH (feet)	INTERVAL (feet)	DESCRIPTION
5222.0	3.1	Limestone; grainstone; light gray; medium grained; fusulinid, pelletoids (?), and misc. skeletal grains; black clay stringers; vuggy porosity.
5225.1	2.5	Limestone; wackestone; gray to light brown; fine to medium grained; phylloid algal and misc. skeletal grains; slight oil stain at base of section.
5227.6	2.0	Limestone; packstone; light brown to gray; fine grained; misc. skeletal grains; vuggy porosity; slight oil stain.
5229.6	3.4	Limestone; wackestone to mudstone; dark gray; fine grained; crinoid and misc. skeletal grains; numerous stylolites; oil stain at base of section.
5233.0	24.0	MISSING SECTION
5257.0	7.9	Limestone; wackestone; dark grey; fine grained; crinoid, misc. skeletal, and algal grains; algal grains horizontally aligned; taxonomic diversity increases down section; stylolites increase in abundance down section; slight oil stain at 5261.8.
5264.9	8.5	Limestone; wackestone to packstone; light to dark gray; fine grained; phylloid algal and misc. skeletal grains; clay laminae (wavy, parallel, continuous); numerous stylolites.
5273.4	0.6	Shaly limestone; wackestone; greenish gray; very fine to fine grained; misc. skeletal grains.

DEPTH (feet)	INTERVAL (feet)	DESCRIPTION
5274.0	1.5	Limestone; wackestone; dark gray; fine grained; mottled bedding; misc. skeletal grains.
5275.5	1.5	Limestone; grainstone; light gray; medium grained; exclusively oolite grains; intraparticle porosity.
5277.0	3.0	Limestone; packstone; gray to brown; fine grained; exclusively phylloid aglal and crinoid grains; vuggy porosity; oil stain associated with vugs and algal grains.
5280.0		END OF CORE

PETROGRAPHIC ANALYSIS  
 Shell Oil Conley 4  
 Conley Field  
 Hardeman County, Texas  
 Palo Pinto Formation

Depth ft	mol %	bra %	for %	pa %	bry %	cri %	int %	oo %	sil %	lm %	pel %	cem %	unk %
5191.0	2	2	0	0	3	10	3	0	0	67	0	10	3
5194.3	3	3	3	0	15	1	23	0	0	48	1	2	3
5196.0	3	2	0	0	3	0	39	0	0	45	0	2	7
5197.5	7	6	7	1	6	2	8	0	0	44	14	2	4
5201.8	1	0	1	0	0	2	54	0	0	41	0	0	1
5209.5	1	7	2	1	4	8	3	0	0	60	1	14	0
5210.5	3	1	0	0	15	21	1	0	11	48	0	0	0
5212.0	1	0	3	0	21	22	3	0	48	0	0	0	1
5214.0	1	1	2	0	10	32	0	0	32	0	0	20	2
5218.0	7	2	3	0	14	8	1	0	62	0	2	0	4
5221.0	13	3	15	1	9	6	13	0	27	0	8	0	6
5223.5	12	6	21	6	0	12	17	0	0	2	5	15	6
5225.5	2	1	8	28	1	1	4	0	0	45	0	10	1
5227.2	4	0	0	33	5	1	4	0	0	38	0	10	5
5229.5	3	2	1	30	3	3	3	0	0	21	0	30	4
5231.5	0	0	2	14	3	5	0	0	0	74	0	0	2
5260.5	4	1	0	16	0	1	16	0	0	23	9	25	4
5261.8	2	4	14	7	10	6	1	0	0	45	2	10	0
5264.0	4	3	2	4	4	7	2	0	0	72	2	1	0
5267.0	0	2	0	2	4	5	28	0	0	38	0	20	2
5268.5	2	0	0	0	1	0	85	0	0	3	0	10	0
5271.5	4	5	2	3	12	12	0	0	0	56	0	5	3
5273.5	2	9	2	0	8	16	6	0	20	38	0	0	0
5275.5	2	1	1	1	2	2	58	0	0	24	6	2	3
5276.0	0	0	0	0	0	0	0	59	0	0	0	40	1
5277.5	0	0	7	2	0	0	2	50	0	0	0	40	0
5278.3	0	0	4	14	0	0	42	0	0	0	0	40	0
5279.5	0	1	3	23	0	1	36	0	0	6	1	25	4

## CORE DESCRIPTION

WELL: Sage Energy Company, Conley 17 (Section 81)  
 FIELD: Conley Field, Hardeman County, Texas  
 FORMATION: Palo Pinto Formation, Canyon Group: Upper  
 Pennsylvanian  
 DEPTH: 5190.0 - 5245.5 feet

DEPTH (feet)	INTERVAL (feet)	DESCRIPTION
5190.0	16.0	Limestone; wackestone; light to dark gray; fine grained; bioturbated; mottled bedding (5190.0 - 5193.0 ft.); crinoid, bryozoan, and misc. skeletal grains; clay laminae (wavy-inclined, subparallel-nonparallel, continuous); calcite spar replaced grains; calcite spar filled vertical fractures; small amount of pyrite replacement of grains.
5206.0	9.0	MISSING SECTION
5215.0	0.4	Limestone; wackestone; light gray; medium grained; bioturbated; high taxonomic diversity; crinoid and fusulinid grains; calcite spar replaced grains.
5215.4	1.4	Limestone; packstone; gray to brown; fine grained; bioturbated; high taxonomic diversity; crinoid, fusulinid, algal, and bryozoan grains; calcite spar replaced grains; vertical spar filled fractures; stylolites; moldic porosity at oil stain; oil stain at 5215.7 - 5216.2 ft.

DEPTH (feet)	INTERVAL (feet)	DESCRIPTION
5216.8	1.2	Limestone; wackestone; light gray; fine grained; bioturbated; abraded skeletal grains; crinoid, fusulinid, and bryozoan grains; clay laminae at bottom of section (wavy, subparallel, continuous); stylolites.
5218.0	1.1	Limestone; packstone; gray; medium grained; bioturbated; fusulinid, crinoid, brachiopod, and phylloid algal grains; calcite spar replaced grains; moldic porosity at 5218.7 - 5219.2 ft.
5219.1	0.9	Limestone; wackestone; gray; fine grained; bioturbated; misc. skeletal, fusulinid, and algal grains; calcite spar replaced grains; stylolite at 5219.3 ft.
5220.0	0.9	Limestone; packstone; light gray; medium grained; bioturbated; fusulinid and algal grains; moldic porosity at 5220.4 ft.; stylolite at 5220.9 ft.
5220.9	4.2	Limestone; wackestone; light to dark gray; fine grained; mottled bedding; crinoid, fusulinid, phylloid algal, and misc. skeletal grains; calcite spar replaced grains; numerous stylolites.
5225.1	0.4	Limestone; packstone; light gray; medium to fine grained; mottled bedding; "channel-fill" of crinoid and fusulinid grains.

DEPTH (feet)	INTERVAL (feet)	DESCRIPTION
5225.5	3.5	Limestone; wackestone; light to dark gray; fine grained; mottled bedding; crinoid, fusulinid, phylloid algal, and misc. skeletal grains; calcite spar replaced grains; stylolites.
5229.0	6.8	Limestone; bafflestone; light gray to white; medium grained; collapse breccia structures; exclusively phylloid algal plates and lime mud; calcite spar occluding primary porosity; moldic porosity; few stylolites.
5235.8	5.4	Limestone; wackestone; light to dark gray (color becomes darker down section); fine grained; bioturbated; mottled bedding; phylloid algal plates increase in abundance up section; crinoid and misc. skeletal grains decrease in abundance up section; clay laminae (wavy, subparallel, continuous); calcite spar replaced grains; stylolites.
5241.2	0.8	Limestone; packstone; light gray; medium grained; bioturbated; fusulinid, crinoid, bryozoan, and brachiopod grains; grains decrease in taxonomic diversity up section; moldic porosity; calcite spar replaced grains.
5242.0	2.0	Limestone; grainstone; tan; medium grained; predominantly oolite grains; fusulinid and misc. skeletal grains; calcite spar partially filled vugs; moldic porosity; oil stain.

DEPTH (feet)	INTERVAL (feet)	DESCRIPTION
5244.0	1.5	Limestone; packstone; gray; fine grained; crinoid, misc. skeletal, and encrusting algal grains; calcite spar partially fill vugs; moldic porosity.
5245.5		END OF CORE

APPENDIX C  
ABBREVIATIONS AND FORMULAS



## ABBREVIATIONS

psig	pounds per square inch
°F	degrees fahrenheit
API	American Petroleum Institute
cf/b	cubic feet per barrel
ppm	parts per million
%	percent
md	millidarcys
in	inches
ft	feet
cm	centimeters
m	meters
μsec/ft	microseconds per foot
BOPD	barrels of oil per day
BBLs	barrels of crude oil
MCF	million cubic feet of gas

=====

mol	Molluscs
bra	brachiopods
for	foraminifera
pa	phyllloid algae
bry	bryozoans
cri	crinoids
int	intraclasts
oo	oolites
sil	siliciclastics
lm	lime mud
pel	pellets
cem	cement
unk	unknown

## FORMULAS

Porosity was calculated from acoustic well logs using the following formula:

$$\emptyset = \frac{\Delta t_r - \Delta t_m}{\Delta t_f - \Delta t_m}$$

Wyllie time-average formula  
(Schlumberger, 1987)

$\emptyset$  = primary porosity

$\Delta t_r$  = sonic log reading =  $\mu\text{sec}/\text{ft}$

$\Delta t_m$  = transit time of matrix = 47.6  $\mu\text{sec}/\text{ft}$

$\Delta t_f$  = transit time of saturating fluid = 189  $\mu\text{sec}/\text{ft}$

=====

The coefficient of correlation (r) was calculated using the following formula:

$$r = \frac{n (\sum xy) - (\sum x) (\sum y)}{\sqrt{[n(\sum x^2) - (\sum x)^2] [n(\sum y^2) - (\sum y)^2]}}$$

r = coefficient of correlation

0.0 = no correlation

0.5 = moderate correlation

1.0 = perfect correlation

n = number of paired observations (thin sections)

x = variable plotted on x-axis (grain type)

y = variable plotted on y-axis (grain type)

## VITA

NAME: Stephen E. Lovell

BIRTHDATE: March 24, 1958

BIRTHPLACE: Harlingen, Texas (USA)

PARENTS: Ms. Norma L. Cowan                      Mr. Leslie G. Lovell  
Austin, Texas                                      Houston, Texas

EDUCATION: University of Texas at Austin  
B.S., Geology (August, 1982)

PROFESSIONAL  
EXPERIENCE: Tenneco Oil Exploration and Production  
Lafayette, Louisiana

Standard Oil Production Company (Sohio)  
Dallas, Texas

PRESENT  
EMPLOYMENT: Tenneco Oil Exploration and Production  
Bakersfield, California

PERMANENT  
ADDRESS: c/o Ms. Norma L. Cowan  
2710 Richcreek  
Austin, Texas 78757